



Original article

Biogenic proficient synthesis of (Au-NPs) via aqueous extract of Red Dragon Pulp and seed oil: Characterization, antioxidant, cytotoxic properties, anti-diabetic anti-inflammatory, anti-Alzheimer and their anti-proliferative potential against cancer cell lines

Najlaa S. Al-Radadi

Department of Chemistry, Faculty of Science, Taibah University, P.O. Box 30002, Al-Madinah Al-Munawarah 14177, Saudi Arabia

ARTICLE INFO

Article history:

Received 29 September 2021

Revised 29 December 2021

Accepted 2 January 2022

Available online 6 January 2022

Keywords:

Green synthesis

Medicinal plant

Antidiabetic Anti-inflammatory

Anti-Alzheimer

Anti-cancer

ABSTRACT

Gold nanoparticles with tiny sizes and biostability are particularly essential and are employed in a variety of biomedical applications. Using a reducing agent and a stabilising agent to make gold nanoparticles has been reported in a number of studies. Gold nanoparticles with a particle size of 25.31 nm were synthesized in this study utilising *Hylocereus polyrhizus* (Red Pitaya) extract, which functions as a reducing and stabilising agent. The extract of Red Pitaya is said to be a powerful antioxidant and anti-cancer agent. Because of its substantial blood biocompatibility and physiological stability, green production of gold nanoparticles with *H. polyrhizus* fruit extract is an alternative to chemical synthesis and useful for biological and medical applications. The formation and size distribution of gold nanoparticles were confirmed by HPLC, UV-Vis spectrophotometer, X-ray diffraction (XRD), Dynamic light scattering (DLS), Zeta potential, Transmission electron microscopy (TEM), Fourier transformed infrared spectroscopy (FTIR), Energy dispersive X-ray (EDX) and X-ray photoelectron spectroscopy (XPS). The well-analysed NPs were used in various biological assays, including anti-diabetic, anti-inflammatory, anti-Alzheimer, and antioxidant (DPPH), and cytotoxic investigations. The NPs also showed a dose-dependent cytotoxic activity against HCT-116, HepG2 and MCF-7 cell lines, with IC_{50} of 100 $\mu\text{g}/\text{mL}$ for HCT-116 cells, 155 $\mu\text{g}/\text{mL}$ for HepG2, and for MCF-7 cells the value was 165 $\mu\text{g}/\text{mL}$ respectively. Finally, the outstanding biocompatibility of Au-NPs has led to the conclusion that they are a promising choice for various biological applications.

© 2022 The Author(s). Published by Elsevier B.V. on behalf of King Saud University. This is an open access article under the CC BY-NC-ND license (<http://creativecommons.org/licenses/by-nc-nd/4.0/>).

1. Introduction

Gold nanoparticles have grown in prominence in recent years because the increased chemical, physical, biological, and optoelectronic properties of the particles are made possible by the technique used to synthesize them, known as green synthesis (Al-Radadi and Adam, 2020). Metal and semiconductor nanoparticles have distinctive size and shape-dependent properties which are very important in many industries (Kamat, 2002; Ocoy et al., 2018). Gold nanoparticles have received great attention in the scientific community because of their unique and powerful Plasmon

resonance peaks in the visible range and because of their potential to be used in biological studies. They are easy to produce, modify, and have properties-dependent on size, shape, and dispersion, therefore metal nanoparticles are popular (Huang, 2006; Khan et al., 2019). NPs have many applications, and gold nanoparticles are considered genuine jewels. While applications for labelling, distribution, heating, and sensing have risen, their significance in biology and/or life sciences is highlighted by the substantial increase in their use, simplicity and environmental friendliness, the use of plant-mediated nanoparticle manufacturing has grown in popularity (Giljohann et al., 2010).

There are many drawbacks to using conventional nanoparticles production techniques (chemical and physical) (Kumar and Yadav, 2009), for example, the use of toxic chemicals, long-term processing, high costs, time-consuming processes, and hazardous by-products (Chang et al., 2021). Green synthesis, on the other hand, is a preferred method for producing nanoparticles owing to its cost efficiency, environmental friendliness, biocompatibility, ease of

E-mail addresses: nsa@taibahu.edu.sa, nsor26@hotmail.com

Peer review under responsibility of King Saud University.



Production and hosting by Elsevier

<https://doi.org/10.1016/j.sjbs.2022.01.001>

1319-562X/© 2022 The Author(s). Published by Elsevier B.V. on behalf of King Saud University.

This is an open access article under the CC BY-NC-ND license (<http://creativecommons.org/licenses/by-nc-nd/4.0/>).

use, and speed of synthesis processes (Herlekar et al., 2014; Simonis and Schilthuisen, 2006). The production of NPs may be carried out by a wide range of organisms, including cyanobacteria, fungi, actinomycetes, and bacteria. As a delivery mechanism for targeted and safer medication distribution, green manufactured nanoparticles provide a potential alternative to cancer medicines. Green synthesis has produced many NPs with distinct biological properties, including Ag, Cu, Au, ZnO, Se, and CuO (Salem et al., 2020; Waris et al., 2021). The main drawback of using plants for green synthesis, is the need for high heating conditions, which raises the cost of nanoparticle manufacturing (Pantidos and Horsfall, 2014). Plant-mediated NP synthesis is a growing trend in green chemistry due to its nontoxic, low-cost, and ease of use (Al-Radadi, 2018; El-Seedi et al., 2019; Manjumeena et al., 2016). Metal oxide nanoparticles (NPs) have seen increased use in the chemical, physical, and biological fields during the last decade (Das and Chatterjee, 2019). With a production rate of 500 tonnes per year and expected to rise in the future, Au-NPs and Ag-NPs stand out as the most promising and marketable NPs (Bindhu and Umadevi, 2014; Al-Radadi (2019)).

A complicated issue, drug resistance affects both developing and developed national healthcare systems. Antibiotic therapies have been decimated by the escalation and spread of diseases that are resistant to several drugs (Aslam et al., 2018). As a result, the search for novel antimicrobial drug sources has intensified recently in order to combat pathogenic diseases that are resistant to it. Medicinal plants and plant-mediated nanomaterials with antimicrobial activities have been extensively studied in this respect, since they cover a broad range of bioactive chemicals with well-established therapeutic characteristics (Talbot et al., 2006). Additionally, Au-NPs have been shown to be effective anti-cancer agents and drug delivery vectors in a variety of cancer cell lines, both in the lab and in the human body. The most prevalent cancers in women are breast cancer and colon cancer. Given its broad distribution, this illness is a major public health concern requiring more molecular and nanoscale investigation in order to ascertain its prognosis and therapeutic possibilities (Manivasagan and Oh, 2015). MCF-7 and HepG2 carcinoma cells may now be effectively treated using plant-derived compounds and nanomaterials produced by plants (Barai et al., 2018). Due to their chemo preventive and less harmful properties, these cancer research molecular weapons are excellent antitumor candidates. These drugs are unable to target a cancer site due to issues such as inadequate solubility and structural deformation, as well as low bioavailability (Vandermeer, 2020; Manikandakrishnan et al., 2019). Recent interest in Au-NPs has been spurred by their innovative therapeutic applications (Vijayan et al., 2018).

Material scientists are now using herbal plants as a stable source for manufacturing metallic nanoparticles as an alternative to conventional methods, considering the aforementioned drawbacks of physical and chemical methods and the use of Au-NPs as a powerful antimicrobial and anti-cancer agent (Katas et al., 2018). The bioconversion of gold ions to nanoparticles was performed using medicinally significant *Hylocereus polyrhizus* aqueous pulp and seed oil extracts. In Mexico, South America, and North America, this plant is readily accessible. In tropical and subtropical areas all over the globe, many dragon fruit species are currently cultivated as fruit orchards. This unique fruit is becoming more popular owing to its peculiar flavour and appearance, as well as its eye-catching colour (Joshi and Prabhakar, 2020; Hua et al., 2018). You can differentiate one type from another by the colour of the pulpy peel or the soft fleshy centre, which contains the seed. The pulpy peel has been shown to have higher antioxidant activity. Due to its scale-like appearance on the outside, the fruit is known as dragon fruit (Al-Mekhlafi et al., 2021). Antioxidant-rich oil was produced from the dragon fruit's small black seeds, which are

found throughout the fruit (Ariffin et al., 2009). Additionally, dragon fruit seeds are a good source of dietary fibre, vitamin C, minerals, carotenoids, phenolic acids, organic acids (including acetic and lactic), protein, flavonoid compounds, phosphorus, iron, and Phyto albumins (a kind of protein) In addition to aiding digestion, the peel and seeds of the dragon fruit reduce cholesterol levels and protect against diabetes and colon cancer by neutralising the harmful effects of heavy metals and other environmental toxins. It is possible to extract the phytoconstituents from the fruit by scraping off the skin and seeds or by using a solvent. The fruit is a good source of betacyanin, vitamins, and lycopene (Utpott et al., 2020; Rebecca et al., 2010). Low-density lipoprotein (LDL) or bad cholesterol (LDL) is protected from oxidation or damage as well as high blood pressure by beta lacin, a red pigment present in the red dragon fruit (Siow and Wong et., 2017; Choo et al., 2016). Anti-hepatitis, burn therapy, anti-microbial, anti-inflammatory, antioxidant, jaundice, and dyspepsia are just a few of the claimed applications for the Dragon Fruit (*Hylocereus polyrhizus*) (Lin et al., 2021; Wu et al., 2006).

We're here to see whether the Au-NPs produced by *Hylocereus polyrhizus* is active against the HepG2, MCF-7, and HCT-116 cell lines, and can it be a viable cancer therapy option for the treatment of breast and colon cancer, respectively. The synthesized NPs were characterized by FTIR, XPS, TEM, XRD, DLS, Zeta potential, and UV. The anti-inflammatory, anti-Alzheimer, anti-diabetic, and antioxidant efficacy of the nanoparticles was also examined (Slepička et al., 2020; Al-Radadi, 2020; Faisal et al., 2021).

2. Materials and methods

2.1. Fruit collection and extraction

Disease-free and healthy fruits of *Hylocereus polyrhizus* were purchased from a local market. To eliminate impurities and dust spores, the collected fruits were rinsed thoroughly using distilled water. The cleaned fruits were peeled and 4.5 g of fruit pulp were blended with 50 mL of distilled water and boiled at 60 °C for 15 min. To remove all residuals, the prepared extract was first twice filtered with nylon paper and then thrice filtered using Whatman filter paper No. 1. The liquid was allowed to cool after filtering before being combined with 10 mL of dragon fruit seed oil (D.pulp _seed oil). For additional tests, the produced extract was retained and refrigerated at 4 °C.

2.2. Biosynthesis of Au-NPs

Established protocol of (Elia et al., 2014), with slight modifications was followed for green synthesis of Au-NPs. Before and after mixing aqueous extract with precursor salt, UV and pH were observed. In short, 50 mL of extract and 10 mL of dragon fruit seed oil were combined with tetra chloroauric acid salt $\text{HAuCl}_4 \cdot 3\text{H}_2\text{O}$ and kept for 4 h at room temperature. The mixture was centrifuged (HERMLE Z326 K) at 10,000 rpm to complete the reaction. The pellet was isolated and rinsed three times with sterile water before being put on autoclaved Petri dish and dried in an

oven at 50 °C. To eliminate contaminants, the dry substance was crushed into powder in a sterile pestle. For further physical characterization and biological applications, the resultant powder NPs were preserved in a sealed glass vial, tagged, and kept refrigerated (Unal et al., 2020).

2.3. Characterization of biosynthesized Au-NPs

Morphological, structural and vibrational properties of biosynthesized Au-NPs were examined using multiple analysis tech-

niques including HPLC, XPS, XRD, DLS, Zeta potential, FTIR, UV and TEM. Phytochemicals and related functional groups on Au-NPs were determined by FTIR spectroscopy (400–4000 cm^{-1}). XRD was used to define the crystal-like nature, phase recognition and purity of Au-NPs (Model-D8 Advance, Germany). Morphological characteristics of NPs were calculated using electron microscopy (TEM). Surface stability and NP size of Au-NPs were explored via (DLS).

2.4. Anti-diabetic assay

A well-established protocol of (Guo et al., 2020) were used for the investigation of antidiabetic potential of biosynthesized nanoparticles. 15 μL of Phosphate buffer saline solution, 25 μL of α -amylase, 10 μL of sample solution and 40 μL of starch were added to 96-wells plate followed by incubation for 30 min at 50 °C. After incubation 20 μL of HCL and 90 μL of iodine were added to each well. Acarbose an antidiabetic drug was used as a positive control while DMSO were used as a negative control. Absorbance were recorded at 540 nm. The percent inhibition was calculated by the following formula

$$\% \text{ Enzyme Inhibition} = \left[1 - \left\{ \frac{\text{Absorbance of sample}}{\text{Absorbance of control}} \right\} \right] \times 100$$

2.5. Anti-inflammatory assay

Cyclooxygenase (COX) are enzymes that forms prostaglandin which induce inflammation, pain, and fever. In this assay biosynthesized gold nanoparticles were investigated to inhibit COX-1 and COX-2 enzymes to reduce inflammation. COX-1 and COX-2 (Ovine kit 701,050 France) were utilized to determine the anti-inflammatory capability of the biosynthesized Au-NPs. 10 mM ibuprofen were used as a positive control. Different concentration of nanoparticles including 50, 100, 200, and 400 $\mu\text{g}/\text{mL}$ were used in the assay inhibition were calculated following the manufacturer instructions. Absorbance were recorded at 590 nm to check N,N,N,N/-tetramethyl-p-phenylene diamine in a 96-well microplate.

2.6. Anti-Alzheimer assay

Acetylcholinesterase (AChE) and Butyrylcholinesterase (BChE) are the two enzymes that has to be targeted and inhibited by the anti-Alzheimer drug in the treatment of Alzheimer disease. The potential of biosynthesized nanoparticles to inhibit AChE (Sigma “101292679”) and BChE (Sigma “101303874”) was determined by using was investigated using Elman’s technique. Nanoparticle concentrations of 25 mg/mL to 400 mg/mL were pre-

pared in PBS. The enzymes concentration was 0.03U/mL AChE and 0.01U/mL BChE and stored at 8°Celsius. Methanolic Galantamine hydrobromide (Sigma; GI660) was used as a positive control, while reaction without any NPs were used as a negative control. 5-thio-2-nitrobenzoate and its complexed with DTNB was formed as a result of hydrolysing ATChI to AChE and BTChI to BChE which results in the formation of yellow colour. The coloured transformed solution was expose to absorbance at 412 nm. The following formula were used to calculate percent enzyme inhibition.

$$V = \Delta \text{Abs} / \Delta t$$

$$\text{Enzyme activity (\%)} = V / V \text{ maximum} \times 100$$

$$\text{Enzyme inhibition (\%)} = 100 - \text{Enzyme activity (\%)}$$

2.7. Antioxidant assay (DPPH)

The 2,2-diphenyl-1-picrylhydrazyl (DPPH) free radical was used to determine the antioxidant action of Au-NPs. The reaction mixture contained 200 $\mu\text{g}/\text{mL}$ concentrations, and the assay was performed thrice. For 30 min at 37 °C, 180 μL of DPPH solution (4.80 $\text{mg}/50 \text{ mL}$ methanol) was combined with a specific amount of 20 μL of test sample from each dose on a 96-well plate. Ascorbic acid was utilized as a positive regulator. Absorbance was measured at 515 nm.

$$\% \text{FRSA} = (1 - \text{Abs}/\text{Abs}) \times 100$$

2.8. Cytotoxicity against HCT-116, HepG2 and MCF-7 cell lines

MCF-7, HCT-116, HepG2, and MCF-7 cells were grown in DMEM with 10% FCS, 100 U/mL penicillin, 2 mM L-glutamine, 100 g/L streptomycin, and 1 mM Na-pyruvate in an ambient atmosphere with 5% humidified CO_2 . The cells were collected for 1 min at room temperature with 0.5 mM trypsin/EDTA. The cytotoxic potential of extracts/nanoparticles was examined in vitro using the tetrazolium dye MTT (3-(4, 5-dimethylthiazol-2-yl) 2, 5-diphenyltetrazolium bromide. A purple, solid material called formazan is formed when MTT is decreased in healthy cells. This substance may be detected spectrophotometrically. In a 96-well plate, pre-seeded cells (>90% viability; 10,000 cells per well) were treated with test substances ranging from 2 to 500 g/mL for 24 h. After that, 10 μL of MTT dye (5 mg/mL) was added to each well and incubated for three hours. To dissolve the insoluble formazan, we employed a 10% acidified sodium dodecyl sulphate solution (SDS). After that, the cells were left to incubate for the duration of the night. A microplate reader read the plate readout at

Table 1

Concentrations of Phenolic, flavonoids, carotenoids, Organic acids and glycosides (mg/g) in Red Dragon Pulp.

Red Dragon Pulp	Phenolic				
	Myricetin	Sinapic	Chlorogenic	Quercetin	Hibiscus acid
	36.55	15.12	9.25	17.45	32.14
Retention time	3.2	11.1	12.4	13.9	15
Red Dragon Pulp	Flavonoids				
	Rutin	Apigenin	Naringin	Kampherol	–
	39.22	19.14	44.12	22.71	–
Retention time	5.4	7.02	9.1	10.4	–
Red Dragon Pulp	Carotenoids				
	β-carotene	Lycopene	Zexanthin	α-carotene	Lutein
	10.25	19.41	11.06	0.39	0.34
Retention time	7.9	10.21	15.00	12.2	13.5
Red Dragon Pulp	Organic acid				
	Succinic acid	Fumaric acid	Ascorbic acid	–	–
	9.56	4.15	16.08	–	–
Retention time	10.01	10.5	11.0	–	–

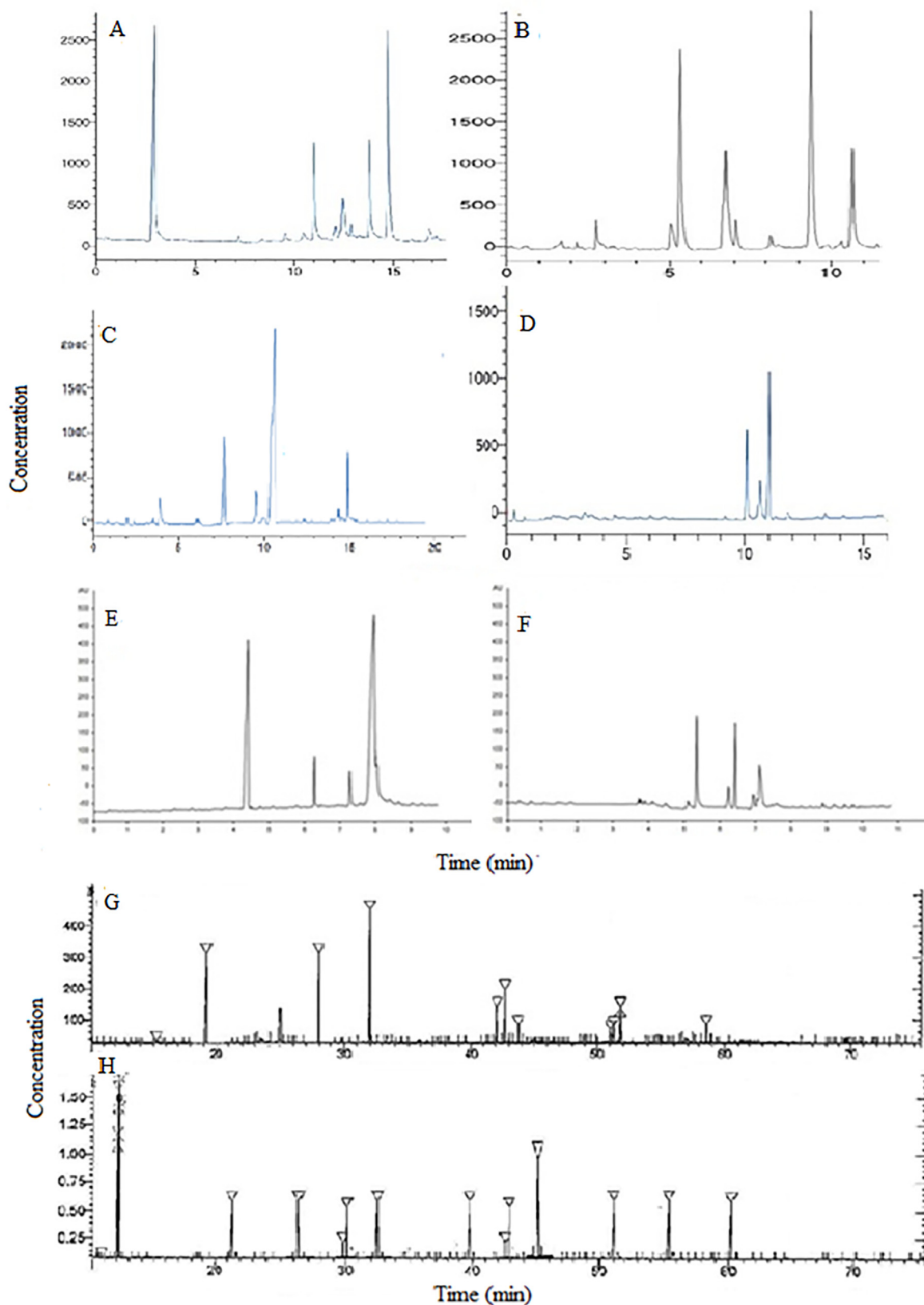


Fig. 1. Analysis of HPLC chromatograms of (A)Phenolic, (B)flavonoids, (C)carotenoids, (D)Organic acids, (E)water-soluble vitamins, (F)fat-soluble vitamins of Red Dragon Pulp and Separation charts (G) Essential Amino Acids, (H)Non-Essential Amino Acids.

Table 2
Concentrations of amino (mg/100 g) in Red Dragon Pulp.

Amino acids				
Red Dragon Pulp	L-Valine	L-Methionine	L-Isoleucine	L-Threonine
	10.33	13.05	5.46	5.13
Retention time	24.8	31.9	27.7	19.2
Red Dragon Pulp	L-Lysine	L-Leucine	Aspartic acid	L-Phenyl alanine
	12.08	8.04	8.37	11.49
Retention time	58.7	51.3	12.6	42.3
Red Dragon Pulp	Alanine	Glycine	Glutamic acid	Arginine
	9.91	18.63	22.19	6.32
Retention time	42.2	40.1	28.9	20.6
Red Dragon Pulp	Cysteine	Histidine	Tyrosine	Proline
	11.42	5.12	5.89	10.06
Retention time	59.7	50.2	58.5	47.6

570 nm (Platos R 496, AMP). DMSO was used as a check against the NPs. Percent viability was calculated using this formula rather than the NTC sample.

$$\% \text{ Viability} = \frac{\text{Absorbance of sample} - \text{Absorbance of samle control}}{\text{Absorbance of NTC} - \text{Absorbance of media}} \times 100$$

3. Results

3.1. Analytical study of Red Dragon Pulp

HPLC analysis revealed the compounds in Dragon Pulp and these including Phenolic, flavonoids, carotenoids, and organic acids were found in differing quantities inside, as indicated in Table 1, as well as in Fig. 1 A- D. Myricetin and hibiscus acid are the most abundant phenolic components in Red Dragon Pulp. Quercetin, Sinapic, and Chlorogenic acid, Rutin, Apigenin, Naringin, and Kaempferol were also found in the Red Dragon Pulp. Analysis revealed that Naringin was the most common flavonoid found in the Red Dragon Pulp. Concentration of (19.14 mg/g) was found to be the lowest for Apigenin. Carotenoids were also found in the Red Dragon Pulp and its five varieties were named accordingly. Lycopene was the most prevalent carotenoid, followed by β -carotene, zeaxanthin, and α -carotene, with lower amounts. L-methionine, L-leucine, and L-valine were all found in the Red Dragon Pulp in high amounts. In Table 2, the levels of the amino acids in the Red Dragon Pulp differed among the various extracts. Aspartic acid and Glycine Methionine were found in significant concentrations in the Red Dragon Pulp, while Isoleucine, Threonine, and Tyrosine were in low concentrations. as in Fig. 1 G,H. GSH and ascorbic acid make up the aqueous phase of antioxidants of the Red Dragon Pulp (ASC) $25.15 \pm 1.71 \mu\text{mol-g}^{-1}$ DW and $39.07 \pm 1.25 \mu\text{mol-g}^{-1}$ DW are detected in these quantities. These results varied from 4.15 mg/g to 16.08 mg/g for the organic acids found in the Red Dragon Pulp. Red Dragon Pulp had the highest amount of ascorbic acid, at 16.08 mg/g. With succinic and fumaric acid, the series concludes. The Red Dragon Pulp also includes various types of vitamins, which may be seen in Table 3 and illustrated

Table 3
Concentrations of vitamins (mg/g) in Red Dragon Pulp.

Vitamins				
Red Dragon Pulp	Vitamin C	Vitamin B₆	Niacin	Cobalamine
	2.84	1.08	0.95	3.51
Retention time	4.4	6.28	7.51	8.02
Red Dragon Pulp	Vitamin E	Vitamin D	Vitamin K	Vitamin A
	2.87	0.35	3.49	2.91
Retention time	5.35	6.12	6.54	7.2

in Fig. 1 E,F. Among analyzed vitamins, nicotinic acid, vitamins k, then vitamins A, vitamins E, vitamin C, vitamin B6, and vitamin D were all had a greater quantity of cobalamin than the other vitamins.

Fatty acids were discovered in various quantities in the Red Dragon Pulp. Typically, the peels have an average fatty acid content of around 0.19 mg/100 g to about 30.94 mg/100 g. In this research, we focused on fatty acids ranging from 100-fold to 1,000-fold of the baseline level, from which baseline fatty acids had been derived (7.28 percent to 30.94 percent). Oleic acid was detected in large quantity of (30.94%) as shown in Table 4, Fig. 2 A-F.

In many essential processes of the human body and creation of high nutritional value, the mineral elements are heavily engaged. Red Dragon Pulp tested in the mineral analysis shown in Table 5 reveals that it is rich in many minerals like calcium, potassium, magnesium, and phosphorus. One of the most critical ingredients was the very high Potassium concentration of (415.9 mg/100 g). It's possible that the primary advantage of dietary potassium is to help keep your blood pressure in check. Additionally, potassium is beneficial in the prevention of stroke and coronary heart disease. Following calcium, these sample's content of Calcium (142.6 mg/100 g) is more. A broad range of studies has shown that

Table 4
Fatty Acid content (%) in Red Dragon Pulp.

Fatty acids			
Red Dragon Pulp	Lauric	Capric	Caprylic
	5.46	0.38	0.67
Retention time	26.1	24.9	22.3
Red Dragon Pulp	Heptadecanoic	Palmitic	Pentadecanoic
	3.26	16.59	2.82
Retention time	31.7	30.2	27.9
Red Dragon Pulp	Linolenic	Linoleic	Oleic
	0.19	2.37	30.94
Retention time	40.04	37.2	35.7
Red Dragon Pulp	Myristic	Lignoceric	Behenic
	9.21	0.23	1.54
Retention time	26.8	43.1	42.3
Red Dragon Pulp	Arachidic	Stearic	-
	7.28	17.48	-
Retention time	39.4	33.8	-

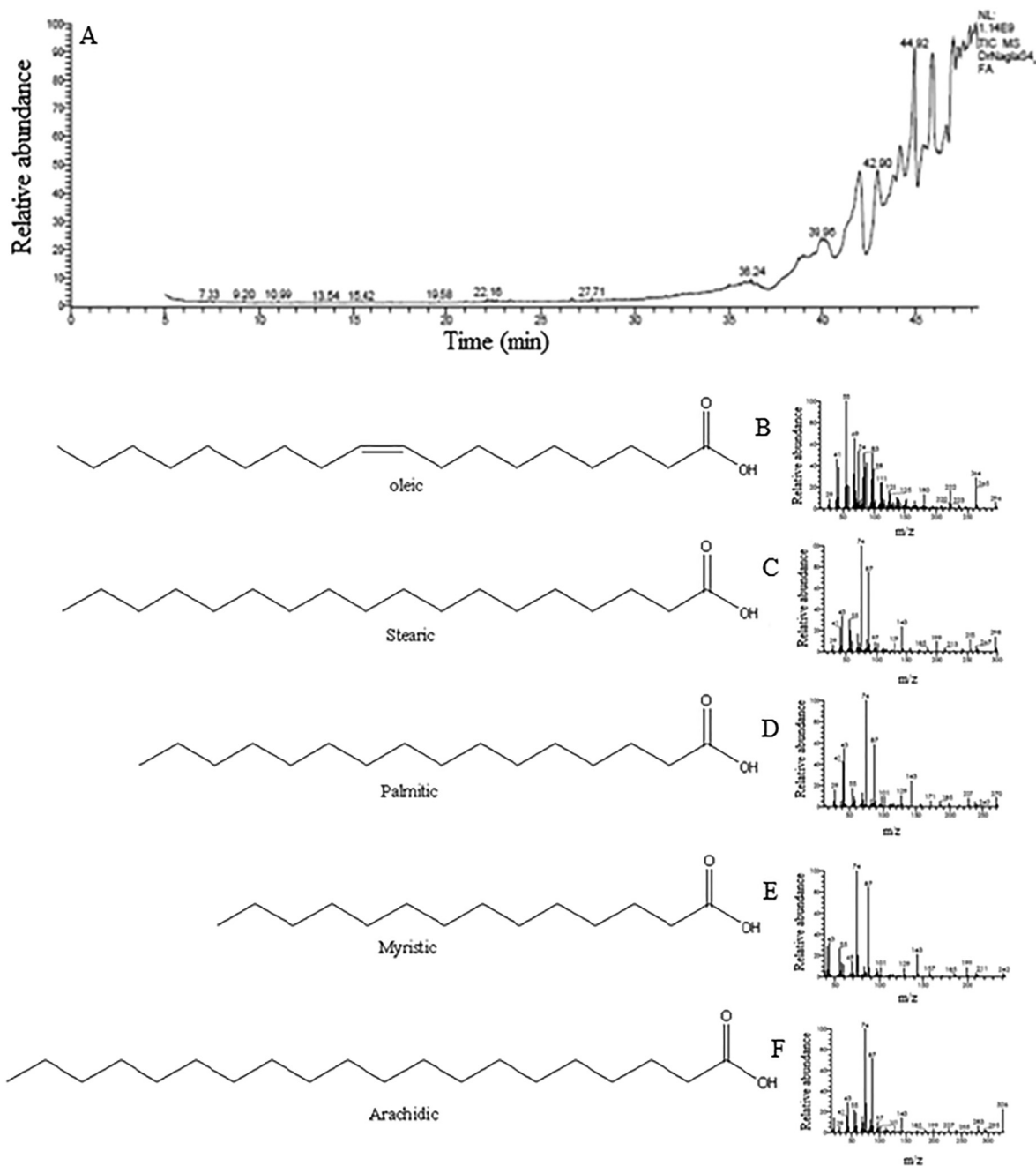


Fig. 2. (A) The chemical chart from Red Dragon pulp HPLC showing the separation of fatty acids and Mass Fragmentation of the separated Compounds (B)Oleic, (C)Stearic, (D) Palmitic, (E)Myristic, (F)Arachidic.

Table 5
Concentrations of minerals (mg/g) in Red Dragon Pulp.

	K	Na	Ca	Cb
Red Dragon Pulp	415.9	3.7	142.6	ND
	Mg	Fe	P	B
	16.4	0.8	57.5	ND
	S	Mn	Zn	Se
	42.8	0.41	0.62	ND

calcium is an effective way to prevent or cure osteoporosis. Additionally, there were some minerals such as Copper, Boron, and Selenium which were found in the pulp, but their amounts are not specified. (See Table 6)

Analysis of phenolic and flavonoid concentration in functional meals may be helpful in determining bioactivity and health benefits. The DPPH free radical scavenging ability of the pulp extracts was evaluated using the reducing power DPPH radicals (µg/ml).

Table 6
Proximate composition (g/100 g or mg/g dry weight) of Red Dragon Pulp.

Proximate Composition					
Red Dragon Pulp	Total Proteins/g/100 g 10.2	Ash g/100 g 12.4	Total Lipids mg/g 22.9	Moisture g/100 g 8.41	Total Carbohydrates g/100 g 35.0

Table 7
Concentrations of sugar (mg/100 g) in Red Dragon Pulp.

sugar					
Red Dragon Pulp	mannose 15.06	Arabinos 5.49	fructose 14.31	Xylose 5.18	
Retention time	6.2	5.3	4.7	3.7	
Red Dragon Pulp	Lactose 11.99	Sucrose 6.97	glucose 9.75	galactose 6.14	
Retention time	9.5	8.8	7.9	7	

In the examination of Red Dragon Pulp of fruit, the findings indicated that the total moisture content was 8.41 g/100 g, protein content was 10.2 g/100 g, ash content was 12.4 g/100 g, and carbohydrate content was 35.0 g/100 g. These findings indicated that, among all the several Red Dragon Pulps studied, the one that had the greatest of vital nutritional elements required for human activities was protein. Contrary to its lipid content, the amount of low-level lipids per gram is much lower. The 8.15% portion of the pulp has both insoluble fiber, and fiber that has been identified and acknowledged as an essential component of human diets (22.3 percent). According to Table 7, the primary sugars found in the pulp were mannose and fructose with amounts of 15.06 mg/g and 14.31 mg/g, respectively. Fructose is considered harmless, with fewer calories than other sugars.

3.2. Biosynthesis of Au-NPs

Hylocereus polyrhizus commonly known as “Dragon fruit” belongs to cactus family that is native to Columbia, Mexico and America. Several type of dragon fruit specie are cultivated as a fruit crop in many tropical and subtropical areas worldwide. The phyto-constituents found in seed oil like betacyanin, vitamins, carotenoids, phenolic, organic acids and lycopene act as a capping and reducing agent. When the reaction is carried out between (*H. polyrhizus* + Respective salts), the color of the solution changes from dark red to dark gray, which confirmed the biosynthesis of Au-NPs. The reaction mixture was centrifuged and stored for physicochemical characterization.

3.3. UV spectroscopy

This analysis was performed to observe the production of Au-NPs. Fig. 3 show the UV-visible spectra of Au-NPs, exhibiting absorption peaks at 540 nm, characteristic of metallic nanoscale gold. The capping of Au-NPs by bioactive elements in the dragon pulp and seed oil extract may explain the change in absorbance from normal at $\lambda_{\max} = 540$ nm (of SPR Au (0)). All these figures depict the spectral data of spectral plasmon resonance vibrations.

3.3.1. The effect of extract volume

A series of reactions was carried out with dragon Pulp_Seed oil extract volumes varying from 1 to 5 mL and a constant amount of $5 \text{ mL } 10^{-3} \text{ M HAuCl}_4 \cdot 3\text{H}_2\text{O}$ as shown in Fig. 3A. The reaction was carried out at room temperature for around 4 h and the color change was observed. UV-visible spectra were taken after 4 h of reactions, and the strength of the SPR peak grew and became sharper as the D. Pulp_Seed oil extract volume increased from 1 mL to 5 mL. As a

result of the optimization research, the amount of extract had a substantial impact on the synthesis of AuNPs@D.pulp_seed oil. This study suggests that extract volume of 5 mL is optimal for nanoparticle formation.

3.3.2. The effect of $\text{HAuCl}_4 \cdot 3\text{H}_2\text{O}$ volume

By synthesizing Au-NPs using different volumes of (1–5 mL) $10^{-3} \text{ M HAuCl}_4 \cdot 3\text{H}_2\text{O}$ and a constant 5 mL of extract at room temperature for 4 h, the optimal volume of $\text{HAuCl}_4 \cdot 3\text{H}_2\text{O}$ was discovered. The UV-vis spectra of 1 mL $\text{HAuCl}_4 \cdot 3\text{H}_2\text{O}$ solution exhibited a low intense peak about 548 nm, which moved to 540 nm with increased intensity when the volume was increased to 5 mL as shown in Fig. 3B.

3.3.3. The effect of pH

By performing the reactions at different pH values ranging from 2, 4, 6, and 8, the influence of pH on the synthesis of AuNPs@D.pulp_seed oil was examined as shown in Fig. 3C. UV was used to monitor the reactions, and the SPR peak at 540 nm confirmed the synthesis of Au-NPs.

Fig. 3C illustrates the UV-visible spectra of AuNPs@D.pulp_seed oil creation, with different pH variables explored. The most favorable pH for D.pulp_seed oil is pH 6 (normal) after 4 h at absorbance of 540 nm, which gives a strength absorbance peak direct to the surface plasmon resonance (SPR Au(0)). Investigating TEM pictures of produced AuNPs@D.pulp_seed oil backs up with the theory that gold nanoparticles are spherical in form, highly dispersed, and non-aggregated, as can be seen in Fig. 4(B). When the pH is raised to 8, the peak intensity increases, but the peak in the UV-vis spectra shift to the right (red shifted $\lambda_{\max} = 577$) as shown in Fig. 3C.

3.3.4. The effect of temperature

A batch of operations was performed at 15 °C, 25 °C, and 35 °C temperature using 5 mL extract and 5 mL $10^{-3} \text{ M HAuCl}_4 \cdot 3\text{H}_2\text{O}$, where the produced Au-NPs reactions were monitored using UV spectra as seen in Fig. 3D. SPR peaks were visible in the UV centred at $\lambda_{\max} = 540$ nm. The strength of absorption peaks grew stronger as time passed from 15 °C to 25 °C, then weakened as time progressed from 25 °C to 35 °C.

3.3.5. The effect of time

At room temperature, a series of procedures were performed using 5 mL extract and 5 mL $10^{-3} \text{ M HAuCl}_4 \cdot 3\text{H}_2\text{O}$ for up to 4 h at 30-minute intervals, UV spectra were used to monitor the reactions of the Au-NPs that were generated. In the UV, SPR peaks were detected at $\lambda_{\max} = 540$ nm. As the reaction time increased, the intensity of the absorption peaks grew stronger, sharper, and

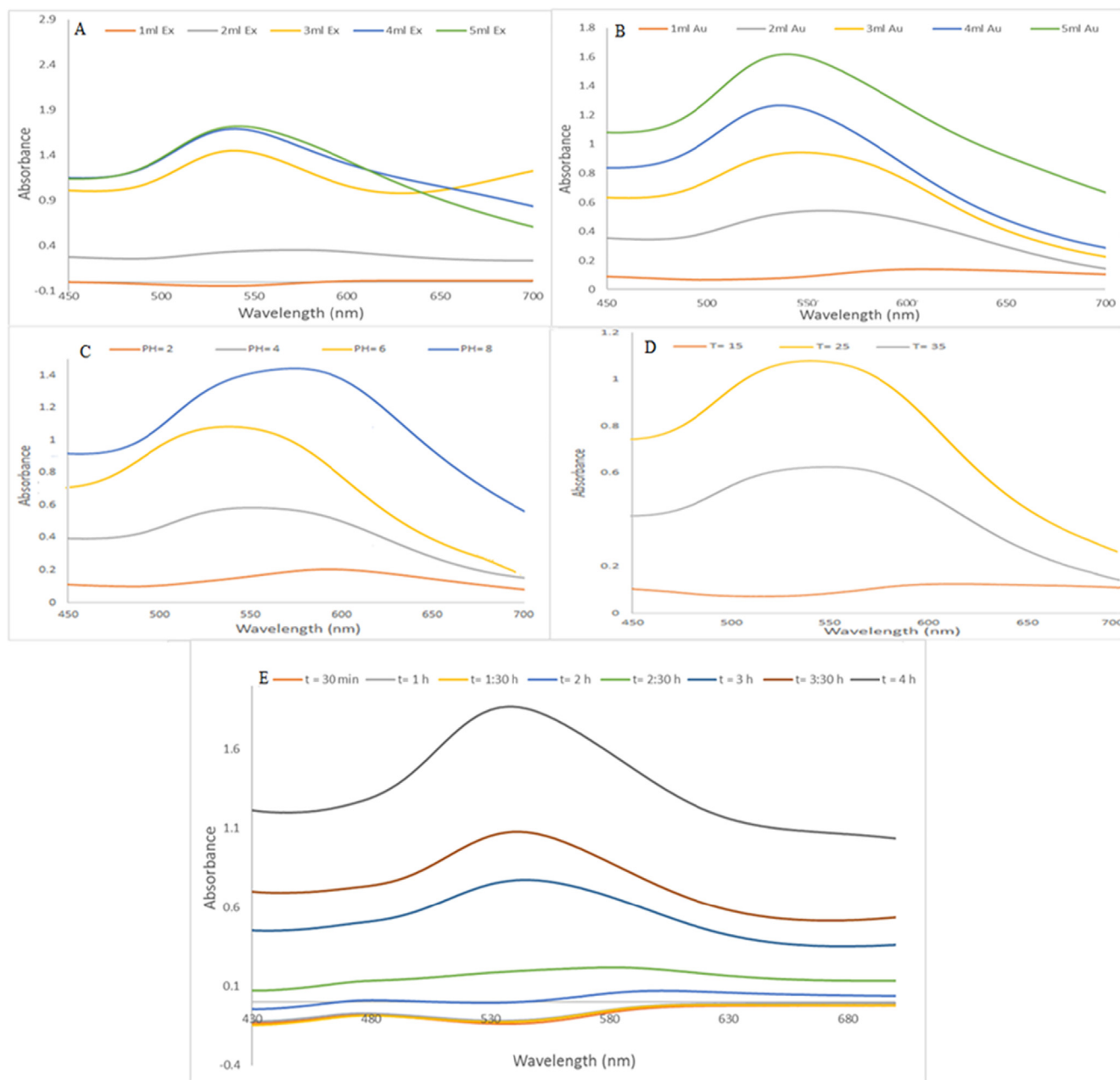


Fig. 3. UV-visible absorption spectra of AuNPs@D.pulp_seed oil synthesized (A) with different volume of (1–5) ml D.pulp_seed oil extract with 5 mL 1×10^{-3} M H_{AuCl₄} stock solutions after 4 h, (B) with different volume of (1–5) ml 1×10^{-3} M H_{AuCl₄} stock solution with 5 mL D.pulp_seed oil extract after 4 h, (C) as a function effect of different (2–8) pH of 5 mL 1×10^{-3} M H_{AuCl₄} stock solution and 5 mL of D.pulp_seed oil extract after 4 h, (D) as a function of 5 mL 1×10^{-3} M H_{AuCl₄} stock solution and 5 mL of D.pulp_seed oil extract with different temperature (15, 25 and 35) °C after 4 h, (E) as a function of 5 mL 1×10^{-3} M H_{AuCl₄} stock solution and 5 mL of D.pulp_seed oil extract with different time of (30–240) minute of addition at 25 °C.

higher, and as time passed, Fig. 3E indicating the best production of Au-NPs at 4 h of reaction time.

3.4. FTIR analysis

FTIR spectra of D.pulp_seed oil and Au-NPs demonstrated that several types of antioxidants were existent in the produced nanoparticles as shown in Fig. 4A. FTIR study was used to inspect the extract and the produced AuNPs@D.pulp_seed oil with a specific goal of identifying present biomolecules in the reduction of the gold ions, such as C = O (which are attributed to carbonyl) and O-H (which are attributed to hydroxyl group). The spectrum shows the

characteristic absorption bands at 3390cm^{-1} broad peak corresponds to the O-H stretch, peak associated with the hydroxyl functional groups of and phenol and alcohol substances found in dragon seed oil extract. The peak at $1765\text{--}1650\text{cm}^{-1}$, which link to C = O absorption band of aliphatic esters and peak at $1385\text{--}1025\text{cm}^{-1}$ correspond to C-O and confirmed the presence of ester bonds in a compound. The band observed in region $3000\text{--}2775$, $1464\text{--}725\text{cm}^{-1}$ recognized to C-H and indicated that long chain aliphatic ester compounds were present. After the encapsulation of nanoparticles, there was a slight shift and variation in intensity was observed in the peaks that clearly indicated the phytochemicals involved in the reduction and stabilization.

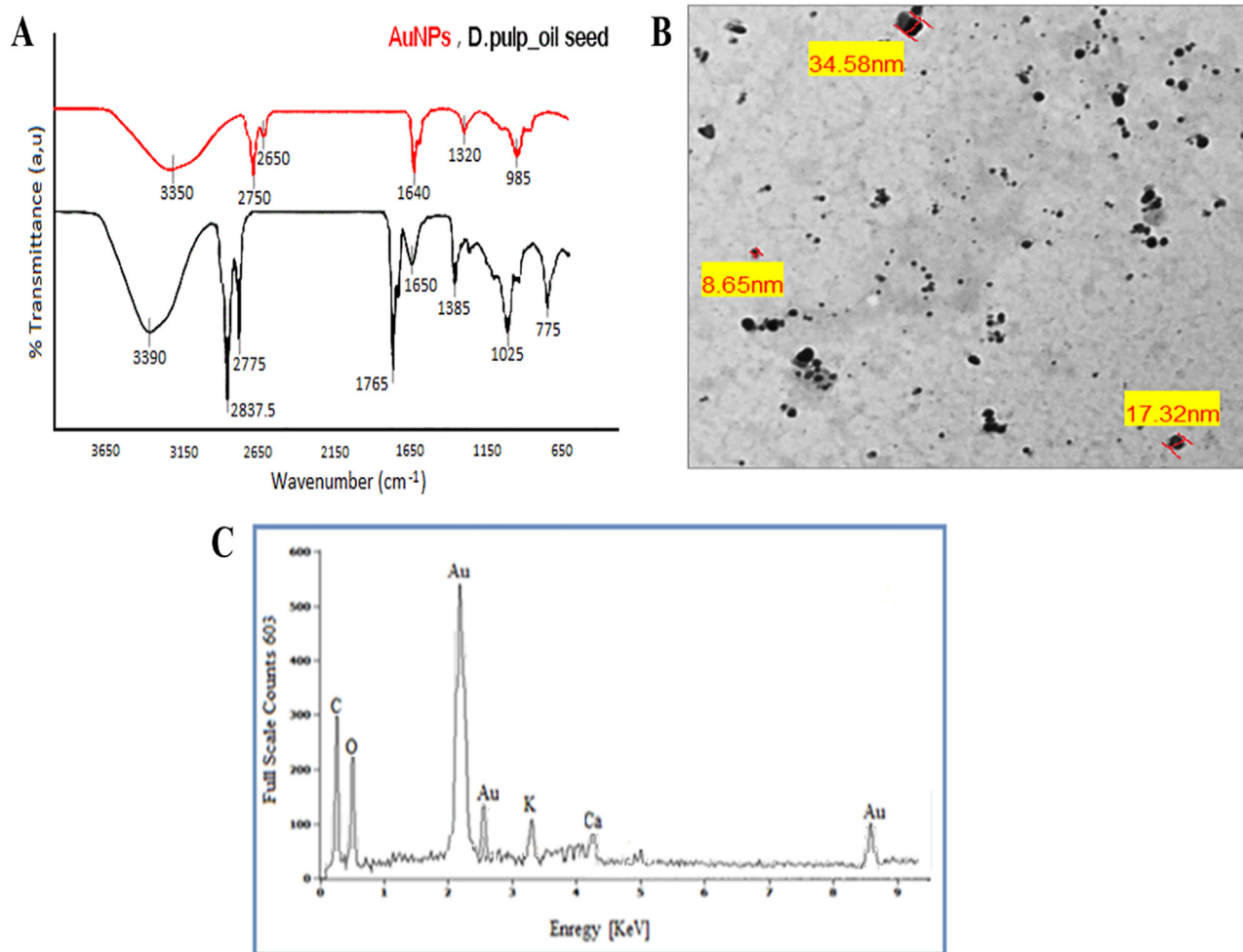


Fig. 4. (A) Typical FTIR analysis of AuNPs@D.pulp_seed oil and respective extract, (B) TEM micrograph of AuNPs@D.pulp_seed oil, (C) EDX spectrum of synthesized AuNPs@D.pulp_seed oil.

3.5. Tem and EDX analysis:

TEM image of Au-NPs is revealed in Fig. 4B. It can be observed that gold nanoparticles are spherical in shape, highly dispersed and non-aggregated with a size distribution from 8.65 to 36.2 nm, effective diameters were measured in 24.9 nm. The obtained gold nanoparticles were verified to contain the gold according to EDX studies. Fig. 4C shows the EDX spectrum of biom-mediated nanoparticles, which confirmed the presence of gold.

3.6. XRD analysis

XRD analysis was used to assess the crystalline state of the gold nanoparticles that were produced. Fig. 5A shows the usual XRD pattern of Au-NPs capped with dragon fruit pulp seed oil extract, demonstrating the crystalline nature of produced Au-NPs. Four unique diffractions peak at 38.29° , 44.22° , 64.77° , and 77.71° are indexed as FCC metallic gold planes (111), (200), (220), and (311). The additional peak of 23.5° in Fig. 5A is due to the extract's amorphous form. The Debye-Scheerer equation $D = K\lambda/\beta \cos \theta$ was used to compute the average size of AuNPs@D.pulp_seed oil.

3.7. DLS analysis

Using Malvern Zeta Sizer, zeta potential and particle size distribution were studied, as shown in Fig. 5B. Zeta potential $|\zeta|$ is a stan-

dard approximation of the surface load that determines the particles' colloidal stability. Suspensions featuring $|\zeta| -18.4$ mV are normally graded as stable colloids. The calculation also improves the stable dispersion potential of biogenic Au-NPs at pH 7 in distilled water as shown in Fig. 5C. The hydrodynamic diameter of the gold nanoparticles prepared using dragon fruit pulp was calculated via DLS technique. DLS analysis is fast and easy techniques. DLS upshot showed that particle size was 36.2 nm.

3.8. X-ray photon spectroscopy

Further to identify the presence of atomic gold and biomolecules around the nanoparticle XPS analysis was performed. Fig. 6 depicts the determined XPS spectra of core levels of the gold i.e. $4f_{5/2}$ and $4f_{7/2}$ at 87.3 and 85.6 BE. Carbon, Nitrogen and Oxygen was presented in Fig. 6B, 6C and 6D respectively. 281.5 BE medium peak was observed and that was due to presence of biomolecular C 1 s (hydrocarbons). A medium peak was observed at 287.2 for BE which lead it to emit electron from C = O and C-OH. A high-flying peak observed at 284.8 and decomposed electron emission of carbonyl carbon. Nitrogen from biomolecules was observed in the triple peak at 396.5, 398.6, and 400.5 BE. Lastly, three O 1 s peaks at 528, 531 NS 533 BE ascribed to the aromatic hydrocarbons in the biomolecules.

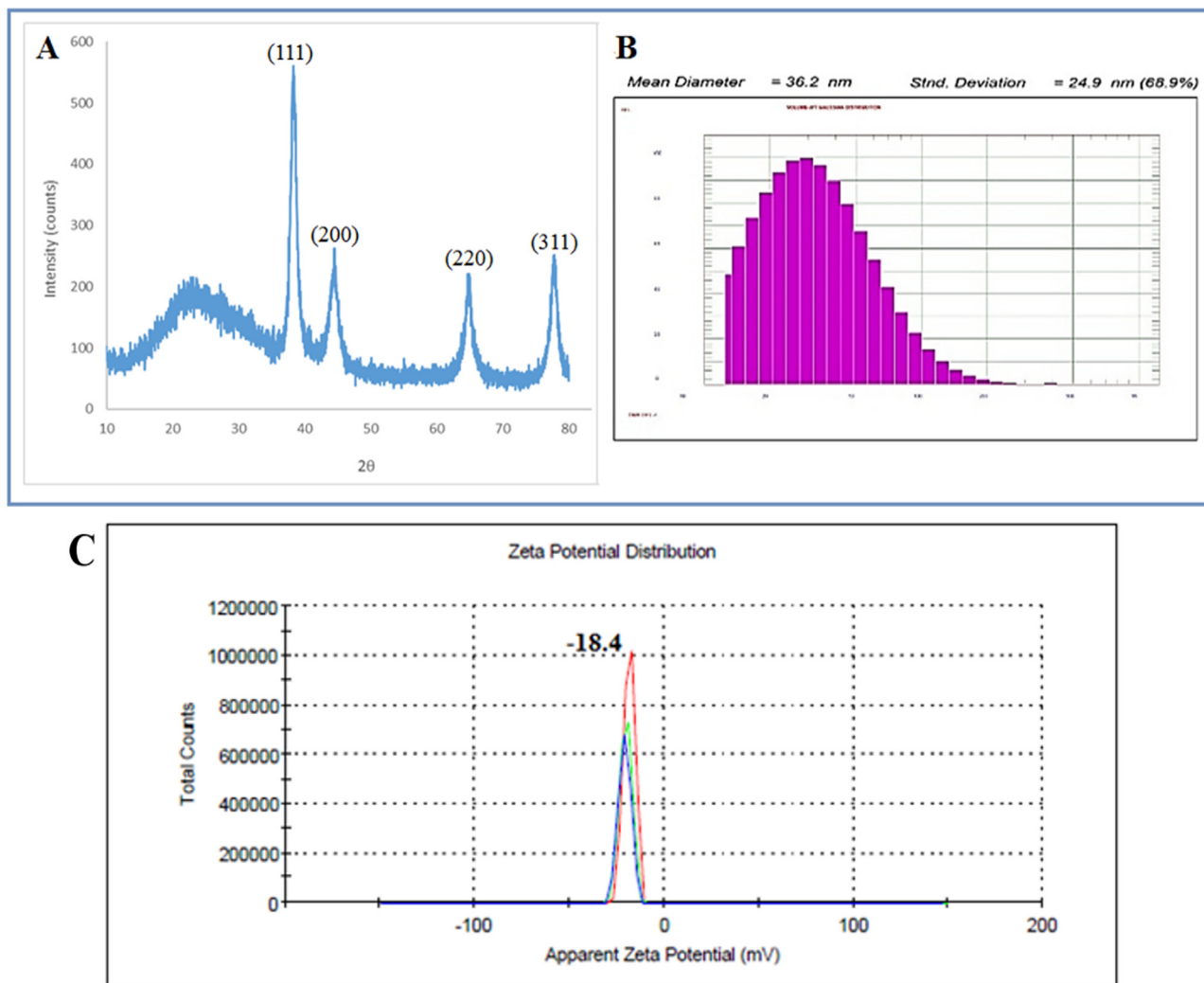


Fig. 5. (A) X-Ray diffraction analysis, (B) DLS zeta size representation, (C) Zeta potential measurements of AuNPs@D.pulp_seed oil.

3.9. Anti-diabetic activity Assay:

Alpha amylase enzyme converts carbohydrates to glucose and thus play an important role in the blood glucose level. Different concentrations of Au-NPs (50 to 200 $\mu\text{g}/\text{mL}$) were used in the assay. Results showed significant inhibition of 40.07 ± 0.65 , 22.02 ± 0.15 , 11.34 ± 0.11 at 200, 100, and 50 $\mu\text{g}/\text{mL}$ respectively as shown in the Table 8 and Fig. 7.

3.10. Anti-inflammatory assay

In Anti-inflammatory assay maximum $50.51 \pm 1.32\%$ inhibition was showed by Au-NPs at a concentration of 400 $\mu\text{g}/\text{mL}$ against COX-1 while $58.74 \pm 0.76\%$ COX-2 inhibition was showed by Au-NPs at same concentration. However, the activity was dose dependent the inhibition increased by the increase of NPs concentration as shown in Table 9 and Fig. 8.

3.11. Anti-Alzheimer assay

In Anti-Alzheimer assay AChE and butrylcholine aryltransferase (BChE) were evaluated at various concentrations of NPs Interestingly, both esterases' inhibitory reaction was depending on the amount of esterase enzyme present. Au-NPs showed significant results at 400 $\mu\text{g}/\text{mL}$ with inhibition of $69.11 \pm 1.12\%$ against AChE

and $64.78 \pm 0.71\%$ against BChE. The inhibition activity was found dose dependent as shown in Table 10 and Fig. 9.

3.12. Antioxidant DPPH assay

The antioxidant activity at different concentrations of 100, 200, 300, 400, and 500 $\mu\text{g}/\text{mL}$ of extract and AuNPs@D.pulp_seed oil was examined by DPPH scavenging assay. In Fig. 10, it is found that the DPPH-scavenging activity increases with the increase in the concentration of D.pulp_seed oil and Au-NPs due inhibition of the interaction with free radical. The D.pulp_seed oil extract and Au-NPs showed a dose-dependent activity and the DPPH scavenging effect was 13 % of D.pulp_seed oil extract and 3% of AuNPs@D.pulp_seed oil at a concentration of 100 $\mu\text{g}/\text{mL}$ and then reached to the 29 % and 9% of D.pulp_seed oil extract and Au-NPs respectively at 500 $\mu\text{g}/\text{mL}$. The activity of the D.pulp_seed oil extract showed much better activity than the Au-NPs. The antioxidant activities of the compounds, present in the extract may depend on structural features, such as the number of phenolic hydroxyl or methoxyl groups and flavones hydroxyl.

3.13. Anti-proliferative assay against HCT-116, HepG2 and MCF-7 Cell:

The vitality of Au-NPs was tested on the MCF-7 breast cancer cell line, HepG2 and the HCT-116 cell line, and it was revealed that

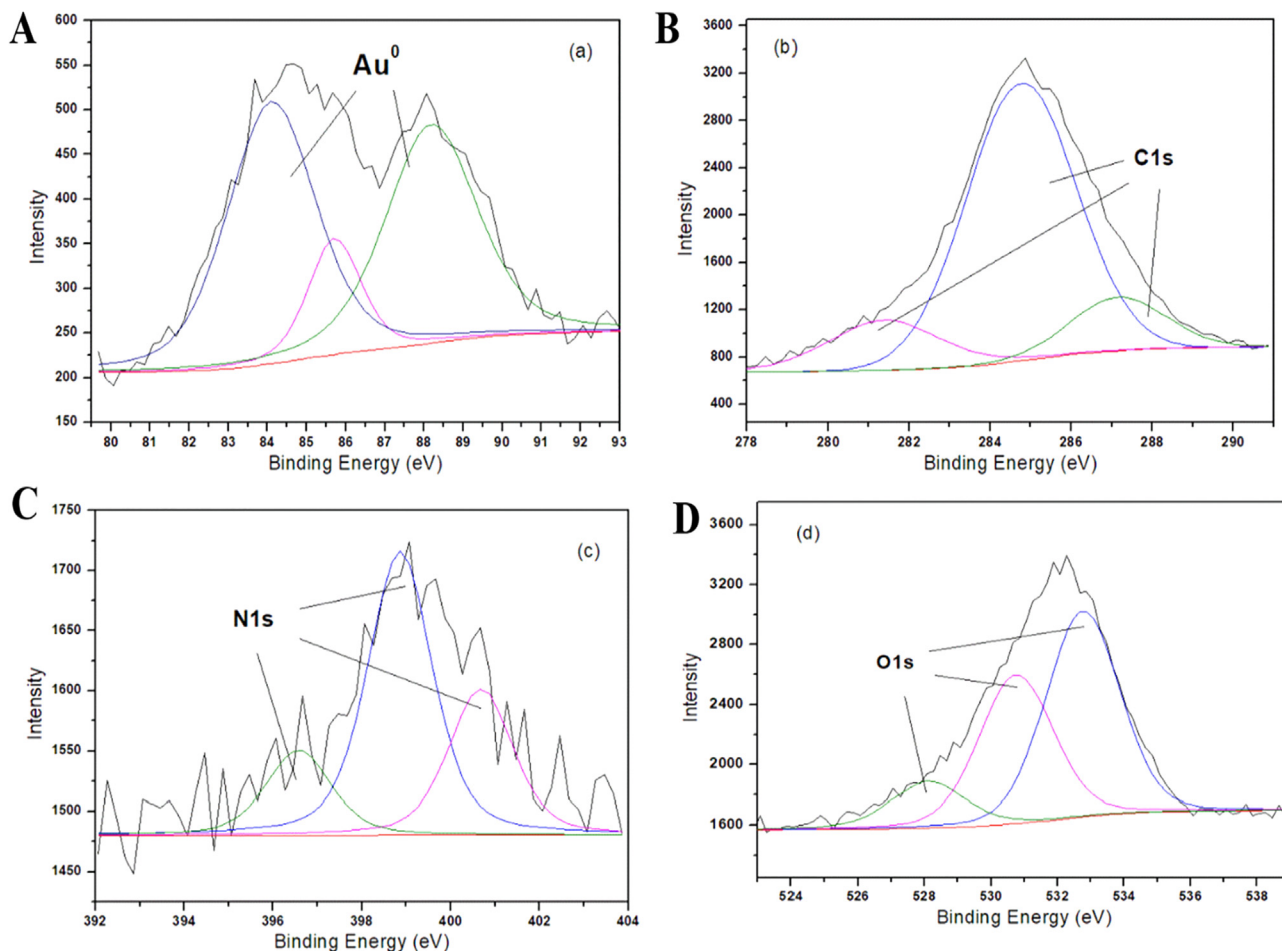


Fig. 6. XPS analysis showing (A) AuNPs@D.pulp_seed oil, (B) C1s, (C) N1s and (D) O1s.

both AuNPs@D.pulp_seed oil and the corresponding extract treatment lowered cell viability. The efficiency and toxicity of D.pulp_seed oil extract derived NPs in MCF-7, HepG2 and HCT-116 cells were investigated. Due to its unique morphological features, Au-NPs demonstrated a greater inhibition of 92.89%, 80.29%, and 74.83% against fresh HCT-116, HepG2, and MCF-7 cell lines at 500 $\mu\text{g/mL}$, similar to antimicrobial activities as shown in Figs. 11–13. MCF-7 had an IC_{50} of 165 $\mu\text{g/mL}$, while HCT-116 had an IC_{50} of 100 $\mu\text{g/mL}$ and HepG2 has an IC_{50} of 155 $\mu\text{g/mL}$. Doxorubicin was utilized as a positive control as shown in Table 11.

4. Discussion

In the preset study gold nanoparticles were synthesized by using D.pulp_seed oil as a capping and reducing agent. The synthesized nanoparticles were characterized by advanced spectroscopic techniques and were evaluated for its biomedical applications. HPLC analysis revealed the compounds in Dragon Pulp and these including Phenolic, flavonoids, carotenoids, and organic acids were found in differing quantities inside. Despite being high in phenolics, the Red Dragon Pulp may nevertheless provide a beneficial contribution to human health owing to its wide range of phenolic chemicals and their use in the treatment of many diseases. Flavonoids and phenolic have been proven itself to provide many healthy advantages, and that including anticancer, anti-inflammatory, anti-diabetes properties, non-toxic, antimicrobial, and antifungal properties (Küp et al., 2020). One study found that lycopene has a preventive effect in many illnesses, such as cancer,

cardiovascular, and neurological disorders. Hence, lycopene was the most prevalent carotenoid, followed by β -carotene, zexanthin, and α -carotene, with lower amounts. L-methionine, L-leucine, and L-valine were all found in the Red Dragon Pulp in high amounts. In small amounts or medium levels of amino acids also existed. It has risen in nutritional value, which contributes to the amino acid content of the Red Dragon Pulp (Al-Radadi, 2019; Wu et al., 2006; Perween et al., 2018). Oleic acid was detected in large quantity of (30.94%) as shown in Table 4, Fig. 2. where it is known that oleic acid helps to reduce cardiovascular disease and especially cholesterol. While limiting saturated fat consumption may be favorable, increasing oleic acid intake can decrease saturated fat intake followed by Stearic acid (17.48%) and finally palmitic acid (16.59 percent) (Fidrianny et al., 2017). In the pulp, phenolics with antioxidant potential were present in large amounts, and their absorption into the extrudates enhanced antioxidant capacity in comparison to controls (Abdullah et al., 2022).

Dragon fruits can be used for nutrition, as well as contain certain therapeutic products such as fibers, vitamin C, minerals, caro-

Table 8
Antidiabetic Assay of Biosynthesized Au-NPs.

Conc. of NPs ($\mu\text{g/mL}$)	% inhibition of α -amylase		
	Au-NPs	Acarbose (100 mg)	DMSO
200	40.07 \pm 0.65	50.10 \pm 0.13	0
100	22.02 \pm 0.15		
50	11.34 \pm 0.11		

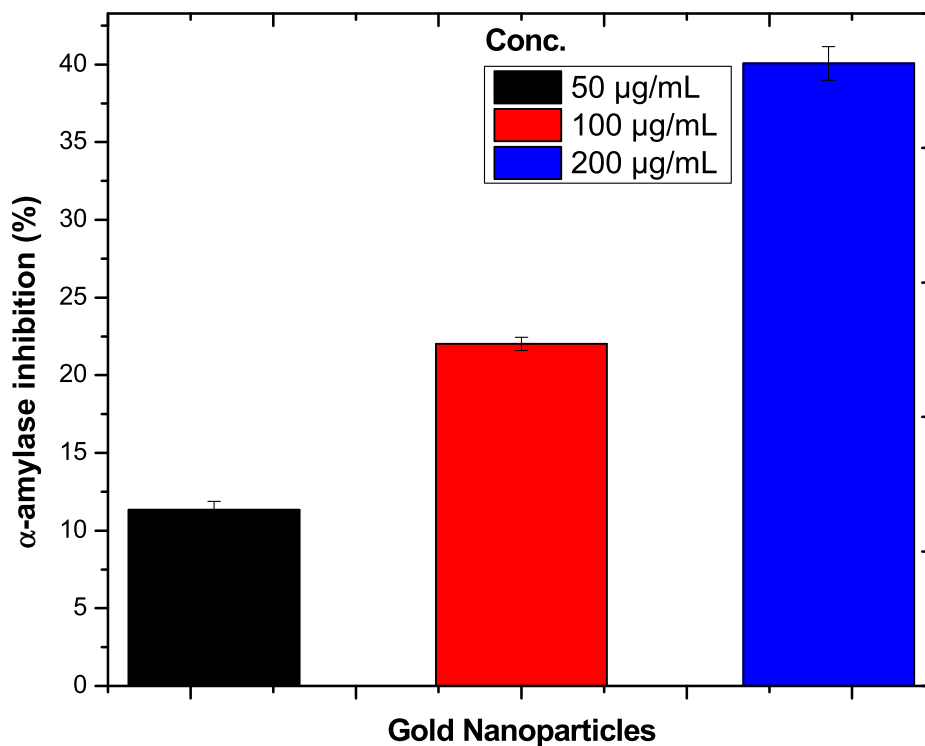


Fig. 7. Anti-diabetic potential of AuNPs@D.pulp_seed oil.

Table 9
Anti-Inflammatory Potential of the AuNPs@D.pulp_seed oil.

Enzymes	NPs	25 $\mu\text{g/mL}$	50 $\mu\text{g/mL}$	100 $\mu\text{g/mL}$	200 $\mu\text{g/mL}$	400 $\mu\text{g/mL}$
COX-1	Au-NPs	8.11 \pm 0.21	15.32 \pm 0.64	29.39 \pm 0.12	36.19 \pm 1.09	50.51 \pm 1.32
COX-2	Au-NPs	13.31 \pm 0.16	19.14 \pm 0.13	31.48 \pm 0.87	31.67 \pm 1.12	58.74 \pm 0.76

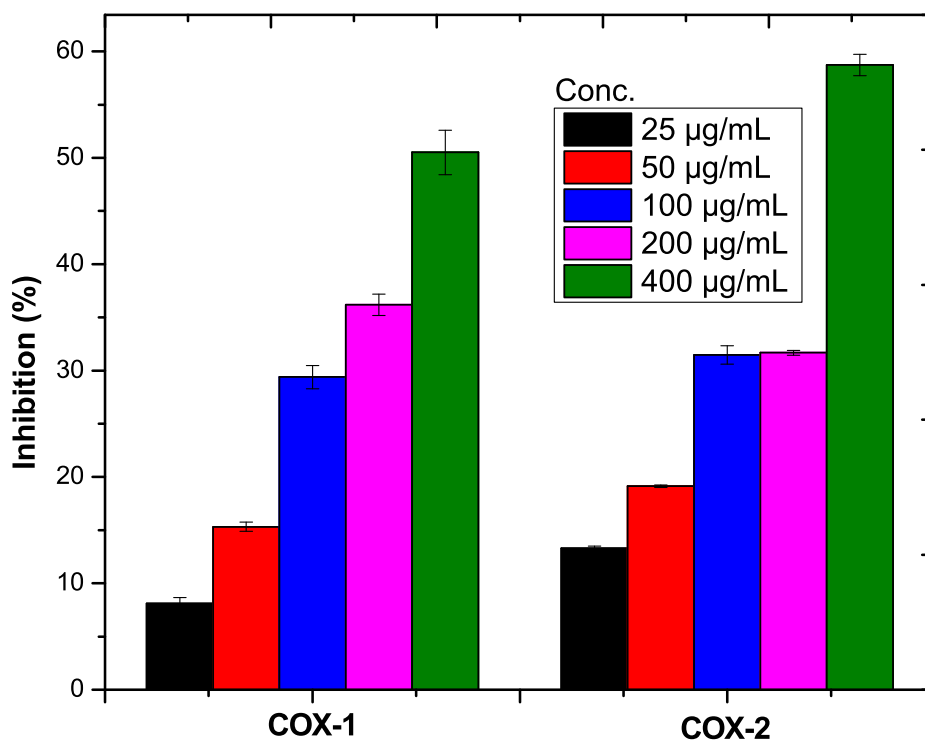


Fig. 8. Anti-inflammatory potential of AuNPs@D.pulp_seed oil.

Table 10
In vitro AChE and BChE inhibition of the AuNPs@D.pulp_seed oil.

Enzymes	NPs	25 µg/mL	50 µg/mL	100 µg/mL	200 µg/mL	400 µg/mL
AChE	Au-NPs	22.81 ± 0.31	28.12 ± 0.54	40.19 ± 0.42	55.19 ± 1.09	69.11 ± 1.12
BChE	Au-NPs	23.11 ± 0.16	33.34 ± 0.13	41.88 ± 0.17	51.17 ± 1.32	64.78 ± 0.71

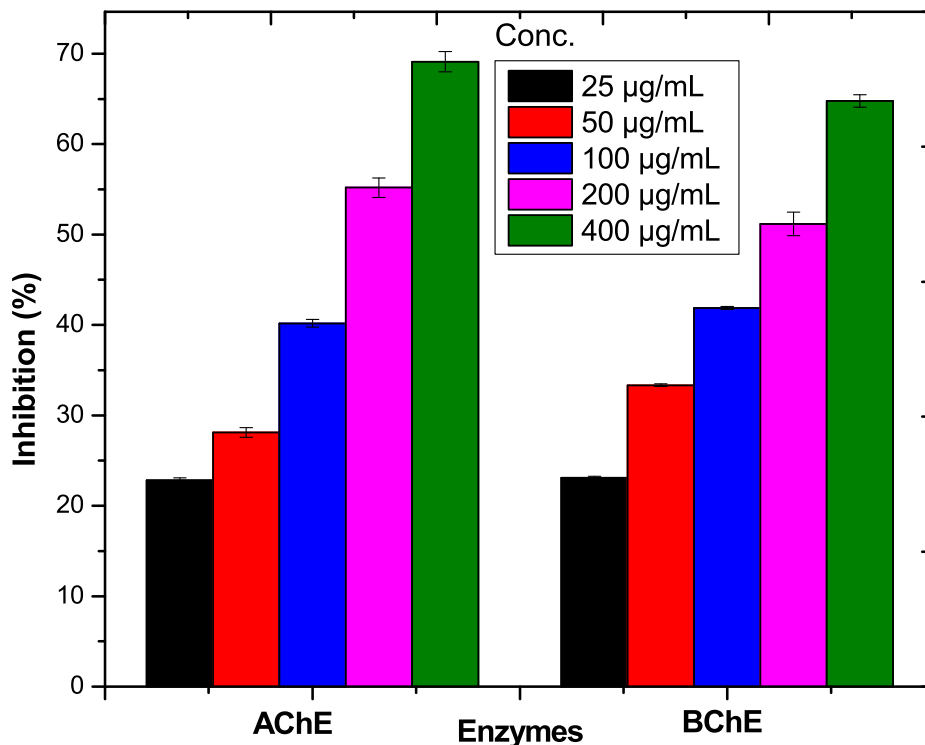


Fig. 9. Anti-Alzheimer potential of AuNPs@D.pulp_seed oil.

tenoids, phenolic, organic acids, protein, flavonoid, phosphorus, iron and phytoalbumins are antioxidant proteins that are highly prized and is well known for their clinical applications, like antimicrobial, anti-inflammatory, antioxidant, jaundice and dyspepsia (Annamalai et al., 2013). UV-visible spectra of AuNPs@D.pulp_seed oil, exhibiting absorption peaks at $\lambda_{max} = 540$ nm, characteristic of metallic nanoscale gold, which is consistent with previous observations (Lee et al., 2011). The spherical and polydisperse character of the AuNPs@D.pulp_seed oil appears to be established by the one wide SPR peak in the spectra (Al-Radadi and Al-Youbi, 2018a). AuNPs@D.pulp_seed oil synthesized with various reaction parameters such as extract volume, metal ion volume at 1×10^{-3} M ($\text{HAuCl}_4 \cdot 3\text{H}_2\text{O}$), pH, and time intervals (Khan et al., 2018; Al-Radadi, 2022). This study suggests that extract volume of 5 mL is optimal for nanoparticle formation, which agrees with the UV-visible absorption study (Kumar et al., 2018). UV-visible and TEM analyses were used to evaluate the synthesized Au-NPs (Wali et al., 2017). production of AuNPs@D.pulp_seed oil, with the peak strength rising as the pH climbed from 2 to 6 (Singh et al., 2018; Ramírez Castro et al., 2018). Peaks of SPR were detected in the UV at $\lambda_{max} = 540$ nm, when the pH was raised to 8, the peak intensity increases, but the peak in the UV-vis spectra shift to the right (Blue shifted $\lambda_{max} = 577$ and become very broad) (Fig. 3C). (Nadaf and Kanase, 2019; Aguilar Pérez et al., 2018). FTIR study was used to inspect the extract and the produced Au-NPs with a specific goal of identifying present biomolecules in the reduction of the gold ions, such as C = O (which are attributed to carbonyl) and O-H

(which are attributed to hydroxyl group) (Santhoshkumar et al., 2017). The peak at $1765\text{--}1650\text{cm}^{-1}$, which link to C = O absorption band of aliphatic esters and peak at $1385\text{--}1025\text{cm}^{-1}$ correspond to C-O and confirmed the presence of ester bonds in a compound (Chaudhuri and Malodia, 2017; Ahmed et al., 2016). Dragon fruit mainly contain betanin, lycopene, and betacyanin. These compositions contain several functional groups that possibly mediate reduction onto Au^{3+} to Au^0 (Syafinar et al., 2015). Gold NPs were designed by the reduction of the respective HAuCl_4 salt ions (Al-Radadi and Al-Youbi, 2018b). XRD analysis was used to assess the crystalline state of the gold nanoparticles that were produced. The additional peak of 23.5° is due to the extract's amorphous form (Khoshnamvand et al., 2020). The band resulting from (111) was sufficiently strong compared to the rest of the planes, indicating that synthesized AuNPs@D.pulp_seed oil are crystalline and that (111) is the primary orientation (Ahmeda, 2020; Khatami et al., 2018). Zeta potential is the standard approximation of the surface polarity that determines the particles' colloidal stability (Al-Radadi, 2021a). DLS analysis is fast and easy techniques. DLS upshot showed that particle size was 36.2 nm. The peak intensity was estimated to be 100 percent (Lee et al., 2015). XPS spectra of core levels of the gold i.e. $4f_{5/2}$ and $4f_{7/2}$ at 87.3 and 85.6 BE (Arunachalam, 2015; Naraginti and Li, 2017). Nitrogen from biomolecules was observed in the triple peak at 396.5, 398.6, and 400.5 BE that can be attributed to the amide nitrogen in the protein (Sportelli et al., 2018; Ali Khan et al., 2021). This clearly indicated that atomic gold was present in nanoparticles and it's capped by

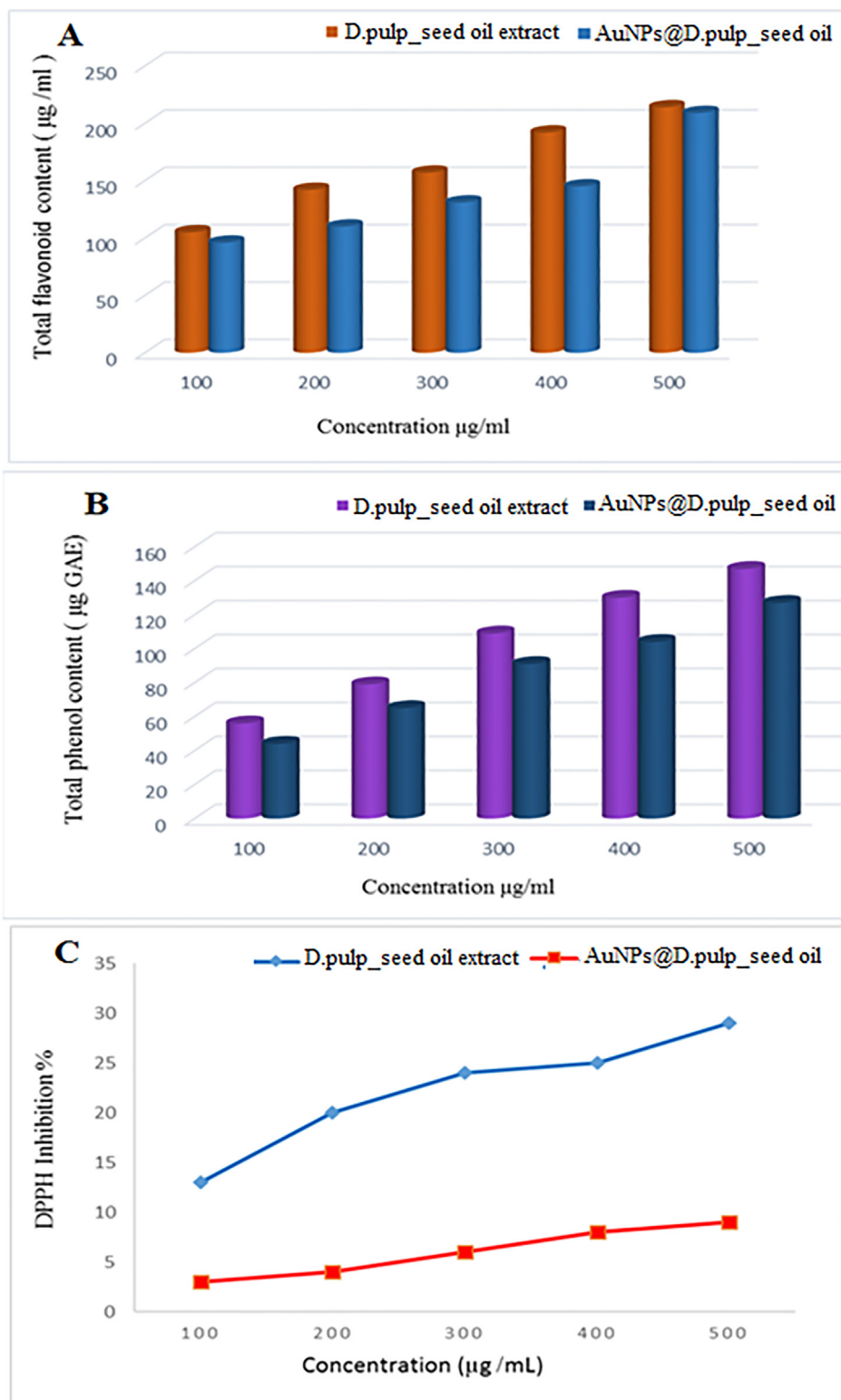


Fig. 10. (A) Total flavonoid of D.pulp_seed oil extract and AuNPs@D.pulp_seed oil at various concentrations (µg/ml), (B) Total phenolic of extract and AuNPs@D.pulp_seed oil at various concentrations (µg/ml), (C) DPPH scavenging activity of extract and AuNPs@D.pulp_seed oil at various concentrations (µg/ml).

the biomolecules in the dragon seed extract (Wu et al., 2015). Results of antidiabetic assay showed significant inhibition of 40.07 ± 0.65 , 22.02 ± 0.15 , 11.34 ± 0.11 at 200, 100, and 50 µg/ml respectively. Alpha amylase enzyme converts carbohydrates to glucose and thus play an important role in the blood glucose level (Kiran et al., 2021; Behzad et al., 2021; Sathishkumar et al., 2018;

Velidandi et al., 2020; Aboyewa et al., 2021). In Anti-inflammatory assay maximum $50.51 \pm 1.32\%$ inhibition was showed by Au-NPs at a concentration of 400 µg/ml against COX-1 while $58.74 \pm 0.76\%$ COX-2 inhibition was showed by Au-NPs at same concentration. White blood cells and the substances they produce have a role in inflammation, which is the body's defence against infection from

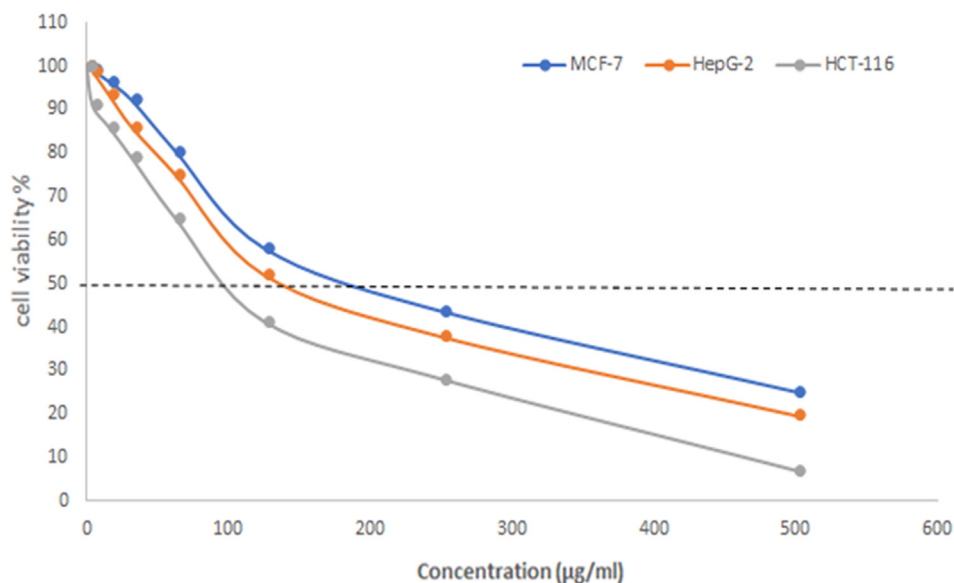


Fig. 11. Cell viability % at different concentrations of AuNPs@D.pulp_seed oil.

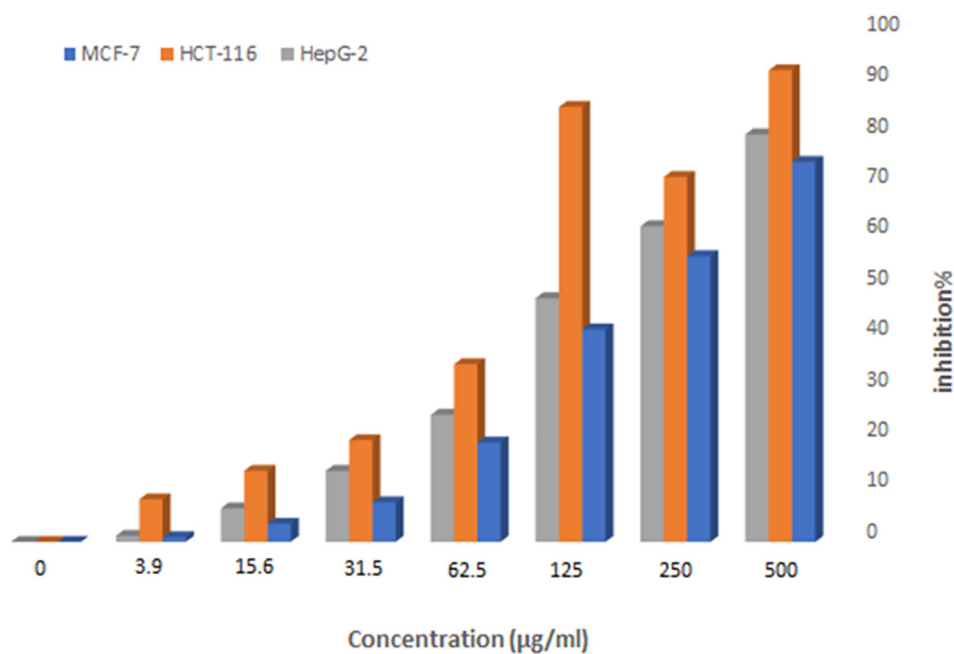


Fig. 12. Inhibitory activity % at different concentrations of AuNPs@D.pulp_seed oil.

outside pathogens, such as bacteria and viruses (Ahn et al., 2018; Paiva-Santos et al., 2021). But sometimes the inflammation gets worsen and effect your body in the form of pain or fever. Au-NPs showed significant inhibition percentage by reducing the inflammation and quenching of COX-1 and COX-2 (Sati et al., 2020; Devasvaran and Lim, 2021; Hosseinikhah et al., 2021; Chen et al., 2017). Over 80% of all dementia cases are the outcome of Alzheimer’s disease. Characterized by a progressive regression of cognitive capacities such as memory, space function, and visuality, personality, and vocabulary, the condition has a peculiar characteristic called cognitive degradation (Youssif et al., 2019). One person gets Alzheimer’s disease every 65 s in the United States alone. 76 Cholinesterase inhibitors are now accessible for the treatment of any degree of Alzheimer’s disease (Bilal et al., 2020). Various syn-

thetic and natural compounds have been published for the purpose of efficient inhibition of cholinesterase enzymes (Kassem et al., 2020). The enzymes function by processing the neurotransmitter acetylcholine into choline and acetic acid at synapses and neuromuscular junctions. AD development can be linked to lower levels of acetylcholine. AuNPs@D.pulp_seed oil showed significant results at 400 µg/mL with inhibition of 69.11 ± 1.12% against AChE and 64.78 ± 0.71% against BChE in anti-Alzheimer assay. As a result of environmental stress, reactive oxygen species (ROS) are produced, which damage membrane lipids, proteins, DNA, and plant cells, causing alterations in plant metabolic pathways (Sergiev et al., 2019). Plants produce a range of metabolic chemicals in response to phenolics, such as flavonoids, terpenoids, and oxidative stress, which activate plant defence mechanisms and are primarily

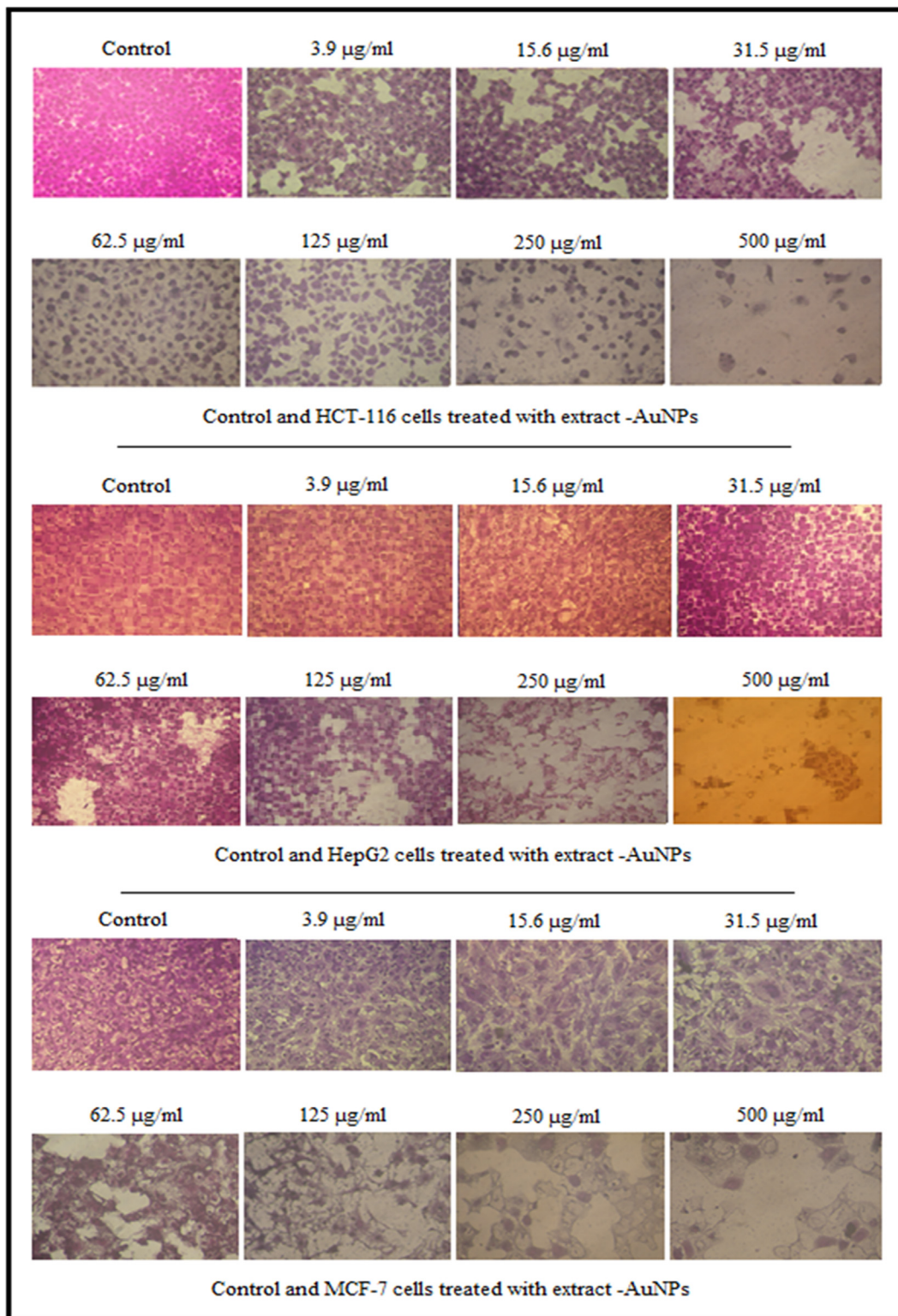


Fig. 13. Effect of synthesized AuNPs@D.pulp_seed oil on morphological assessment of HCT-116, HepG2 and MCF-7 cells.

involved in the production of flavonoids, terpenoids, and oxidative stress (Mohamed and Akladious, 2017; Rehman et al., 2017). Numerous studies have confirmed the positive link between phenolic component concentration and antioxidant capacity of fruits, as well as the reduction of H₂AuCl₄ to AuNPs@D.pulp_seed oil. Antioxidants serve an important function in preventing free radical damage to cells, which is hazardous to human health. Recently, the

intake of natural materials, such as fruits with antioxidant activity, has grown (Francis et al., 2018). The key variables involved in pathogenicity are reactive oxygen species and other free radicals produced during diverse biological activities. As you may be aware, antioxidant substances are defined as any chemical that prevents or reduces oxidative damage to cells. DPPH is a test for determining antioxidant characteristics of any substance ability to decrease free

Table 11
Anti-proliferative potential of synthesized AuNPs@D.pulp_seed oil against HCT-116, HepG2 and MCF-7 cell lines.

Sample Conc. ($\mu\text{g/ml}$)	HCT-116 Cell viability % Inhibitory activity %		IC ₅₀	HepG2 Cell viability % Inhibitory activity %		IC ₅₀	MCF-7 Cell viability % Inhibitory activity %		IC ₅₀
	Stand.	Sample		Stand.	Sample		Stand.	Sample	
	500	9.60		7.11 92.89	100		17.48	19.71 80.29	
250	17.28	28.12 71.88	$\mu\text{g/ml}$	29.45	37.82 62.18	$\mu\text{g/ml}$	17.64	43.69 56.31	
125	31.36	41.32 58.68		45.69	52 48		20.82	58.16 41.84	
62.5	44.45	65 35		55.95	75 25		41.96	80.44 19.56	
31.5	58.64	80 20		71.33	86 14		49.40	92.21 7.79	
15.6	64.40	86 14		75.50	93.40 6.6		54.12	96.44 3.56	
3.9	69.34	91.61 8.39		78.92	98.81 1.19		60.21	99.10 0.9	
0	100	100 0		100	100 0		100	100 0	

radicals. The DPPH radical is purple in hue, but as it is diminished, it turns yellow, and absorption is lost. It assesses antioxidant activity and free radical scavenging. DPPH is a stable free radical with a nitrogen core that takes electrons or hydrogen atoms from antioxidant materials. DPPH is a well-known method for assessing antioxidant activity due to its ability to decrease free radicals. When the DPPH is reduced, the colour changes to yellow, this is because of the anti-oxidative compounds that provide hydrogen to DPPH (Zayadi et al., 2019; Chahardoli et al., 2018). Qualitative phytochemical analysis of D.pulp_seed essential oil was conducted and the tests revealed that D.pulp_seed essential oil has contained 214 $\mu\text{g/mL}$ of flavonoids and 147 $\mu\text{g/mL}$ of phenolic compounds in 00 $\mu\text{g/mL}$, which was the highest used concentration of D.pulp_seed essential oil. The total flavonoids and phenolic compounds in Au-NPs were 209 $\mu\text{g/mL}$ and 142 $\mu\text{g/mL}$, respectively, as shown in Fig. 10. DPPH-scavenging activity was increased with the increase in the concentration of D.pulp_seed oil and Au-NPs due to inhibition of free radicals (Veerakumar et al., 2014). The D.pulp_seed oil and Au-NPs have shown a dose-dependent activity and the observed DPPH scavenging effect was 13 % for D.pulp_seed oil and 3% for AuNPs@D.pulp_seed oil at a concentration of 100 $\mu\text{g/mL}$. The scavenging activity was raised up to 29 % and 9% for D.pulp_seed oil and AuNPs@D.pulp_seed oil respectively at 500 $\mu\text{g/mL}$. The synthesized Au-NPs have also shown a good capacity of scavenging the DPPH free radicals (Vijayan et al., 2018). The most prevalent malignancy among women is breast cancer. Because of its broad impact, this illness is a major public health concern that requires additional molecular and nanotechnology research to establish prognosis and therapy possibilities (Selim and Hendi, 2012). Plant-derived compounds and nanomaterials have lately been praised as a promising and practical alternative for treating MCF-7 and other cancer cells (Barai et al., 2018). These anticancer compounds are less toxic and chemo-preventive, making them a hotspot for cancer research. However, they are restricted in their ability to target a cancer site due to issues such as inadequate solubility, structural deformation, and bioavailability (Manikandakrishnan et al., 2019). Because of their sophisticated medicinal uses, AuNPs@D.pulp_seed oil has sparked a lot of attention recently (Oueslati et al., 2020). In Anticancer assay MCF-7 had an IC₅₀ of 165 $\mu\text{g/mL}$, while HCT-116 had an IC₅₀ of 100 $\mu\text{g/mL}$ and HepG2 has an IC₅₀ of 155 $\mu\text{g/mL}$. Doxorubicin was utilized as a positive control (Heim and Mitelman, 2015). Most evidence for in vitro

activity, on the other hand, is based on nature and the availability of compounds in plant extracts that may be utilised as effective capping agents (Badeggi et al., 2020). Overall, our results provide solid evidence to back up previous research (Parveen and Rao, 2015; Balasubramanian et al., 2020). According to anticancer activity testing findings, biogenic AuNPs@D.pulp_seed oil exhibit potent anticancer effects on colon cancer cells (Al-Radadi, 2021b; Suganthi et al., 2018). The total absorption, elimination, and anti-tumour activities of the test materials are influenced by physical characteristics, surface chemistry, and dosage dependency. Metallic NPs produce DNA damage, which causes malignant cells to die, according to some sources, although the exact mechanism of NPs cytotoxicity remains unknown. The functional group interaction of cellular proteins with NPs, which leads to DNA damage, was also described as a method of Ag and Au NPs cytotoxicity (Al-Radadi, 2021b; Han et al., 2018; Botcha and Prattipati, 2020). Our research also found that Au-NPs may cause oxidative stress by generating reactive oxygen species (ROS), and ROS can cause DNA damage and cancer cell death (Baghbani-Arani et al., 2017).

In general, gold nanoparticles have the potency to be used in the biomedical activities. However in vivo studies must be designed to know about the exact cytotoxicity of the bio inspired AuNPs@D.pulp_seed oil.

5. Conclusion

Gold nanoparticles were successfully synthesised utilising D.pulp_seed oil extract as the initial reducing and stabilising agent in this study. HPLC, UV, XRD, FTIR, TEM, EDX, DLS, Zeta potential, and XPS investigations have all been used to analyse and characterize the water-soluble gold nanoparticles. Gold nanoparticles may be synthesised and stabilised by using chemical reduction process. Preventing diabetes and colon cancer with D.pulp_seed oil is only one of the many benefits of using this supplement. Antioxidant, anti-diabetic, anti-inflammatory, anti-Alzheimer and anti-cancer effects are all found in D.pulp_seed oil. D.pulp_seed oil extract mediated gold nanoparticles have shown remarkable results in research on anti-diabetic, anti-inflammatory, anti-Alzheimer, and anti-cancer properties. HCT-116, HepG2 and MCF-7 cell lines were all killed by the cytotoxic effects of the NPs and extracts. This study's findings on gold nanoparticles produced from D.pulp_seed oil extract shown that they may be used

as a vectors in biomedical applications such as medication administration, gene delivery, or as biosensors where they will come into contact with blood.

Funding

No fund was taken from any source.

Declaration of Competing Interest

The authors declare that they have no known competing financial interests or personal relationships that could have appeared to influence the work reported in this paper.

References

- Abdullah, Al-Radadi, N.S., Hussain, T., Faisal, S., Ali Raza Shah, S., 2022. Novel Biosynthesis, Characterization and Bio-catalytic Potential of Green Algae (*Spirogyra hyalina*) Mediated Silver Nanomaterials. *Saudi J. Biol. Sci.* 29 (1), 411–419. <https://doi.org/10.1016/j.sjbs.2021.09.013>.
- Aboyewa, J.A., Sibuyi, N.R., Meyer, M., Oguntibeju, O.O., 2021. Green Synthesis of Metallic Nanoparticles Using Some Selected Medicinal Plants from Southern Africa and Their Biological Applications. *Plants* 10 (9), 1929.
- Aguilar Pérez, B., García-Hernández, L., Ramírez Ortega, P.A., Arenas Islas, D., 2018. Green synthesis of gold nanoparticles (AuNPs) using the extract of *Sedum praealtum*. *ECS Trans.* 84 (1), 321–330.
- Ahmed, S., Annu, Ikram, S., Yudha S., 2016. Biosynthesis of gold nanoparticles: A green approach. *J. Photochem. Photobiol.*, B 161, 141–153. <https://doi.org/10.1016/j.jphotobiol.2016.04.034>.
- Ahn, E.-Y., Hwang, S.J., Choi, M.-J., Cho, S., Lee, H.-J., Park, Y., 2018. Upcycling of jellyfish (*Nemopilema nomurai*) sea wastes as highly valuable reducing agents for green synthesis of gold nanoparticles and their antitumor and anti-inflammatory activity. *Artif. Cells Nanomed. Biotechnol.* 46 (sup2), 1127–1136.
- Ali Khan, S., Bakhsh, E.M., Asiri, A.M., Bahadar Khan, S., 2021. Synthesis of zero-valent Au nanoparticles on chitosan coated NiAl layered double hydroxide microspheres for the discoloration of dyes in aqueous medium. *Spectrochim. Acta Part A Mol. Biomol. Spectrosc.* 250, 119370. <https://doi.org/10.1016/j.saa.2020.119370>.
- Al-Mekhlafi, N.A., Mediani, A., Ismail, N.H., Abas, F., Dymerski, T., Lubinska-Szczygeł, M., Vearasilp, S., Gorinstein, S., 2021. Metabolomic and antioxidant properties of different varieties and origins of Dragon fruit. *Microchem. J.* 160, 105687. <https://doi.org/10.1016/j.microc.2020.105687>.
- Al-Radadi, N.S., 2018. Artichoke (*Cynara scolymus* L.), Mediated Rapid Analysis of Silver Nanoparticles and Their Utilisation on the Cancer Cell Treatments. *J. Comput. Theor. Nanosci.* 15 (6), 1818–1829.
- Al-Radadi, N.S., 2019. Green synthesis of platinum nanoparticles using Saudi's Dates extract and their usage on the cancer cell treatment. *Arabian J. Chem.* 12 (3), 330–349.
- Al-Radadi, N.S., 2021a. Facile one-step green synthesis of gold nanoparticles (AuNP) using licorice root extract: Antimicrobial and anticancer study against HepG2 cell line. *Arabian J. Chem.* 14 (2), 102956. <https://doi.org/10.1016/j.arabj.2020.102956>.
- Al-Radadi, N.S., 2021b. Green Biosynthesis of Flaxseed Gold Nanoparticles (Au-NPs) as Potent Anti-cancer Agent Against Breast Cancer Cells. *J. Saudi Chem. Soc.* 25 (6), 101243. <https://doi.org/10.1016/j.jscs.2021.101243>.
- Al-Radadi, N.S., 2022. Microwave Assisted Green Synthesis of Fe@Au Core-Shell NPs Magnetic to Enhance Olive oil Efficiency on Eradication of *Helicobacter pylori* (Life preserver). *Arabian J. Chem.* <https://doi.org/10.1016/j.arabj.2022.103685>.
- Al-Radadi, N.S., Adam, S.I.Y., 2020. Green biosynthesis of Pt-nanoparticles from Anbara fruits: Toxic and protective effects on CCl4 induced hepatotoxicity in Wister rats. *Arabian J. Chem.* 13 (2), 4386–4403.
- Al-Radadi, N.S., Al-Youbi, 2018a. One-Step Synthesis of Au Nano-Assemblies and Study of Their Anticancer Activities. *J. Comput. Theor. Nanosci.* 15 (6), 1861–1870.
- Al-Radadi, N.S., Al-Youbi, 2018b. Environmentally-Safe Synthesis of Gold and Silver Nano-Particles with AL-Madinah Barni Fruit and Their Applications in the Cancer Cell Treatments. *J. Comput. Theor. Nanosci.* 15 (6), 1853–1860.
- Annamalai, A., Christina, V.L.P., Sudha, D., Kalpana, M., Lakshmi, P.T.V., 2013. Green synthesis, characterization and antimicrobial activity of Au NPs using *Euphorbia hirta* L. leaf extract. *Colloids Surf., B* 108, 60–65.
- Ariffin, A., Bakar, J., Tan, C., Rahman, R., Karim, R., Loi, C., 2009. Essential fatty acids of pitaya (dragon fruit) seed oil. *Food* 114 (2), 561–564.
- Aslam, B., Wang, W., Arshad, M.I., Khurshid, M., Muzammil, S., Rasool, M.H., et al., 2018. Antibiotic resistance: a rundown of a global crisis. *Infect. Drug Resistance* 11, 1645.
- Badeggi, U., Ismail, E., Adeloye, A., Botha, S., Badmus, J., Marnewick, J., Cupido, C., Hussein, A., 2020. Green synthesis of gold nanoparticles capped with Procyanidins from *Leucosidea sericea* as potential antidiabetic and antioxidant agents. *Biomolecules* 10 (3), 452. <https://doi.org/10.3390/biom10030452>.
- Baghban-Arani, F., Movagharnia, R., Sharifian, A., Salehi, S., Shandiz, S.A.S., 2017. Photo-catalytic, anti-bacterial, and anti-cancer properties of phyto-mediated synthesis of silver nanoparticles from *Artemisia tournefortiana* Rchb extract. *J. Photochem. Photobiol., B* 173, 640–649.
- Balasubramanian, S., Kala, S.M.J., Pushparaj, T.L., 2020. Biogenic synthesis of gold nanoparticles using *Jasminum auriculatum* leaf extract and their catalytic, antimicrobial and anticancer activities. *Journal of Drug Delivery Science and Technology.* 57, 101620. <https://doi.org/10.1016/j.jddst.2020.101620>.
- Barai, A.C., Paul, K., Dey, A., Manna, S., Roy, S., Bag, B.G., Mukhopadhyay, C., 2018. Green synthesis of *Nerium oleander*-conjugated gold nanoparticles and study of its in vitro anticancer activity on MCF-7 cell lines and catalytic activity. *Nano Converg.* 5 (1). <https://doi.org/10.1186/s40580-018-0142-5>.
- Behzad, F., Naghib, S.M., kouhbanani, M.A.J., Tabatabaei, S.N., Zare, Y., Rhee, K.Y., 2021. An overview of the plant-mediated green synthesis of noble metal nanoparticles for antibacterial applications. *J. Ind. Eng. Chem.* 94, 92–104.
- Bilal, M., Barani, M., Sabir, F., Rahdar, A., Kyzas, G.Z., 2020. Nanomaterials for the treatment and diagnosis of Alzheimer's disease. *NanoImpact* 20, 100251. <https://doi.org/10.1016/j.impact.2020.100251>.
- Bindhu, M.R., Umadevi, M., 2014. Silver and gold nanoparticles for sensor and antibacterial applications. *Spectrochim. Acta Part A Mol. Biomol. Spectrosc.* 128, 37–45.
- Botcha, S., Prattipati, S.D., 2020. Callus extract mediated green synthesis of silver nanoparticles, their characterization and cytotoxicity evaluation against MDA-MB-231 and PC-3 Cells. *BioNanoScience.* 10 (1), 11–22.
- Chahardoli, A., Karimi, N., Sadeghi, F., Fattahi, A., 2018. Green approach for synthesis of gold nanoparticles from *Nigella arvensis* leaf extract and evaluation of their antibacterial, antioxidant, cytotoxicity and catalytic activities. *Artif. Cells Nanomed. Biotechnol.* 46 (3), 579–588.
- Chang, Y., Zheng, C., Chinnathambi, A., Alahmadi, T.A., Alharbi, S.A., 2021. Cytotoxicity, anti-acute leukemia, and antioxidant properties of gold nanoparticles green-synthesized using *Cannabis sativa* L leaf aqueous extract. *Arabian J. Chem.* 14 (4), 103060. <https://doi.org/10.1016/j.arabj.2021.103060>.
- Chaudhuri, S.K., Malodia, L., 2017. Biosynthesis of zinc oxide nanoparticles using leaf extract of *Calotropis gigantea*: characterization and its evaluation on tree seedling growth in nursery stage. *Appl. Nanosci.* 7 (8), 501–512.
- Chen, P.C., Tsai, W.J., Ueng, Y.F., Tzeng, T.T., Chen, H.L., Zhu, P.R., Li, W.T., 2017. Neuroprotective and anti-neuroinflammatory effects of hydroxyl-functionalized stilbenes and 2-Arylbenzo [b] furans. *J. Med. Chem.* 60 (9), 4062–4073.
- Choo, J., Koh, R., Ling, A., 2016. Medicinal properties of pitaya: a review. *Spatula DD.* 6 (2), 1. <https://doi.org/10.5455/spatula.10.5455/spatula.20160413015353>.
- Das, M., Chatterjee, S., 2019. Green synthesis of metal/metal oxide nanoparticles toward biomedical applications: Boon or bane. *Green Synthesis, Characterization and Applications of Nanoparticles*: Elsevier. *Micro and Nano Technologies*, 265–301. <https://doi.org/10.1016/B978-0-08-102579-6.00011-3>.
- Devasvaran, K., Lim, V., 2021. Green synthesis of metallic nanoparticles using pectin as a reducing agent: a systematic review of the biological activities. *Pharm. Biol.* 59 (1), 494–503.
- Elia, P., Zach, R., Hazan, S., Kolusheva, S., Ze, P., Zeiri, Y., 2014. Green synthesis of gold nanoparticles using plant extracts as reducing agents. *Int. J. Nanomed.* 9, 4007.
- El-Seedi, H.R., El-Shabasy, R.M., Khalifa, S.A.M., Saeed, A., Shah, A., Shah, R., Iftikhar, F.J., Abdel-Daim, M.M., Omri, A., Hajrahand, N.H., Sabir, J.S.M., Zou, X., Halabi, M. F., Sarhan, W., Guo, W., 2019. Metal nanoparticles fabricated by green chemistry using natural extracts: biosynthesis, mechanisms, and applications. *RSC Adv.* 9 (42), 24539–24559.
- Faisal, S., Al-Radadi, N.S., Jan, H., Abdullah, Shah, S.A., Shah, S., Rizwan, M., Afshen, Z., Hussain, Z., Uddin, M.N., Idrees, M., Bibi, N., 2021. Curcuma longa Mediated Synthesis of Copper Oxide, Nickel Oxide and Cu-Ni Bimetallic Hybrid Nanoparticles: Characterization and Evaluation for Antimicrobial, Anti-Parasitic and Cytotoxic Potentials. *Coatings* 11 (7), 849. <https://doi.org/10.3390/coatings11070849>.
- Fidrianny, I., Ilham, N., Hartati, R., 2017. Antioxidant profile and phytochemical content of different parts of super red dragon fruit (*Hylocereus costaricensis*) collected from West Java-Indonesia. *Asian J. Pharm. Clin. Res.* 10 (12), 290. <https://doi.org/10.22159/ajpcr.2017.v10i12.21571>.
- Francis, S., Koshy, E.P., Mathew, B., 2018. Green synthesis of *Stereospermum suaveolens* capped silver and gold nanoparticles and assessment of their innate antioxidant, antimicrobial and antiproliferative activities. *Bioprocess Biosyst. Eng.* 41 (7), 939–951.
- Giljohann, D., Seferos, D., Daniel, W., Massich, M., Patel, P., Mirkin, C., 2010. Gold nanoparticles for biology and medicine. *Angew. Chem. Int. Ed.* 49 (19), 3280–3294.
- Guo, Y., Jiang, N., Zhang, L., Yin, M., 2020. Green synthesis of gold nanoparticles from *Fritillaria cirrhosa* and its anti-diabetic activity on Streptozotocin induced rats. *Arabian J. Chem.* 13 (4), 5096–5106. <https://doi.org/10.1016/j.arabj.2020.02.009>.
- Han, C., Yang, J., Gu, J., 2018. Immobilization of silver nanoparticles in Zr-based MOFs: Induction of apoptosis in cancer cells. *J. Nanopart. Res.* 20, 1–11.
- Heim, S., Mitelman, F., 2015. Cancer cytogenetics: chromosomal and molecular genetic aberrations of tumor cells. *John Wiley & Sons*.
- Herlekar, M., Barve, S., Kumar, R., 2014. Plant-mediated green synthesis of irker nanoparticles. *J. Nanopart.* 2014, 1–9. <https://doi.org/10.1155/2014/140614>.
- Hosseinihah, S.M., Barani, M., Rahdar, A., Madry, H., Arshad, R., Mohammadzadeh, V., Cucchiari, M., 2021. Nanomaterials for the Diagnosis and Treatment of Inflammatory Arthritis. *Int. J. Mol. Sci.* 22 (6), 3092.

- Hua, Q., Chen, C., Tel Zur, N., Wang, H., Wu, J., Chen, J., Zhang, Z., Zhao, J., Hu, G., Qin, Y., 2018. Metabolomic characterization of pitaya fruit from three red-skinned cultivars with different pulp colors. *Plant Physiol. Biochem.* 126, 117–125.
- Huang, S.-H., 2006. Gold nanoparticle-based immunochromatographic test for identification of *Staphylococcus aureus* from clinical specimens. *Clin. Chim. Acta* 373 (1–2), 139–143.
- Joshi, M., Prabhakar, B., 2020. Phytoconstituents and pharmaco-therapeutic benefits of pitaya: A wonder fruit. *J. Food Biochem.* 44 (7). <https://doi.org/10.1111/jfbc.v44.710.1111/jfbc.13260>.
- Kamat, P.V., 2002. Photophysical, photochemical and photocatalytic aspects of metal nanoparticles. *J. Phys. Chem. B* 106 (32), 7729–7744.
- Kassem, L.M., Ibrahim, N.A., Farhana, S.A., 2020. Nanoparticle Therapy Is a Promising Approach in the Management and Prevention of Many Diseases: Does It Help in Curing Alzheimer Disease? *J. Nanotechnol.* 2020, 1–8.
- Katas, H., Moden, N.Z., Lim, C.S., Celesistinus, T., Chan, J.Y., Ganasan, P., et al., 2018.. Biosynthesis and potential applications of silver and gold nanoparticles and their chitosan-based nanocomposites in nanomedicine. *J. Nanotechnol.* <https://doi.org/10.1155/2020/8147080>.
- Khan, S., Bakht, J., Syed, F., 2018. Green synthesis of gold nanoparticles using *Acer pentapomicum* leaves extract its characterization, antibacterial, antifungal and antioxidant bioassay. *Dig. J. Nanomater. Biostroct.* 13, 579–589.
- Khan, T., Ullah, N., Khan, M.A., Mashwani, Z.-u.-R., Nadhman, A., 2019. Plant-based gold nanoparticles; a comprehensive review of the decade-long research on synthesis, mechanistic aspects and diverse applications. *Adv. Colloid Interface Sci.* 272, 102017. <https://doi.org/10.1016/j.cis.2019.102017>.
- Khatami, M., Sharifi, I., Nobre, M.A.L., Zafarnia, N., Aflatoonian, M.R., 2018. Waste-grass-mediated green synthesis of silver nanoparticles and evaluation of their anticancer, antifungal and antibacterial activity. *Green Chem. Lett. Rev.* 11 (2), 125–134.
- Khosnamvand, M., Hao, Z., Huo, C., Liu, J., 2020. Photocatalytic degradation of 4-nitrophenol pollutant and in vitro antioxidant assay of gold nanoparticles synthesized from *Apium graveolens* leaf and stem extracts. *Int. J. Environ. Sci. Technol.* 17 (4), 2433–2442.
- Kiran, M.S., Kumar, C.R., Shwetha, U.R., Onkarappa, H.S., Betageri, V.S., Latha, M.S., 2021. Green synthesis and characterization of gold nanoparticles from *Moringa oleifera* leaves and assessment of antioxidant, antidiabetic and anticancer properties. *Chem. Data Collect.* 33, 100714.
- Kumar, P.V., Kala, S.M.J., Prakash, K.S., 2018. Synthesis of gold nanoparticles using *Xanthium Strumarium* leaves extract and their antimicrobial studies: a green approach. *Rasayan J. Chem.* 11 (4), 1544–1551.
- Kumar, V., Yadav, S.K., 2009. Plant-mediated synthesis of silver and gold nanoparticles and their applications. *J. Chem. Technol. Biotechnol.: Int. Res. Process. Environ. Clean Technol.* 84 (2), 151–157.
- Küp, F.Ö., Coşkunçay, S., Duman, F., 2020. Biosynthesis of silver nanoparticles using leaf extract of *Aesculus hippocastanum* (horse chestnut): Evaluation of their antibacterial, antioxidant and drug release system activities. *Mater. Sci. Eng., C* 107, 110207.
- Lee, J., Kim, H.Y., Zhou, H., Hwang, S., Koh, K., Han, D.-W., Lee, J., 2011. Green synthesis of phytochemical-stabilized Au nanoparticles under ambient conditions and their biocompatibility and antioxidative activity. *J. Mater. Chem.* 21 (35), 13316. <https://doi.org/10.1039/c1jm11592h>.
- Lee, K.D., Nagajyothi, P.C., Sreekanth, T.V.M., Park, S., 2015. Eco-friendly synthesis of gold nanoparticles (AuNPs) using *Inonotus obliquus* and their antibacterial, antioxidant and cytotoxic activities. *J. Ind. Eng. Chem.* 26, 67–72.
- Lin, X., Gao, H., Ding, Z., Zhan, R., Zhou, Z., Ming, J., 2021. Comparative Metabolic Profiling in Pulp and Peel of Green and Red Pitayas (*Hylocereus polyrhizus* and *Hylocereus undatus*) Reveals Potential Valorization in the Pharmaceutical and Food Industries. *BioMed research international.* 2021, 2021. <https://doi.org/10.1155/2021/6546170>.
- Manikandakrishnan, M., Palanisamy, S., Vinosha, M., Kalanjiraja, B., Mohandoss, S., Manikandan, R., Tabarsa, M., You, SangGuan, Prabhu, N.M., 2019. Facile green route synthesis of gold nanoparticles using *Caulerpa racemosa* for biomedical applications. *J. Drug Deliv. Sci. Technol.* 54, 101345. <https://doi.org/10.1016/j.jddst.2019.101345>.
- Manivasagan, P., Oh, J., 2015. Production of a Novel Fucoidanase for the Green Synthesis of Gold Nanoparticles by *Streptomyces* sp. and Its Cytotoxic Effect on HeLa Cells. *Journal of the Marine. Drugs* 3 (11), 6818–6837. <https://doi.org/10.3390/md13116818>.
- Manjumeena, R., Venkatesan, R., Duraibabu, D., Sudha, J., Rajendran, N., Kalaichelvan, P.T., 2016. Green nanosilver as reinforcing eco-friendly additive to epoxy coating for augmented anticorrosive and antimicrobial behavior. *Silicon* 8 (2), 277–298.
- Mohamed, H.I., Akladios, S.A., 2017. Changes in antioxidants potential, secondary metabolites and plant hormones induced by different fungicides treatment in cotton plants. *Pesticide biochemistry and physiology* 142, 117–122. <https://doi.org/10.1016/j.pestbp.2017.04.001>.
- Nadaf, N.Y., Kanase, S.S., 2019. Biosynthesis of gold nanoparticles by *Bacillus marisflavi* and its potential in catalytic dye degradation. *Arabian Journal of Chemistry.* 12 (8), 4806–4814. <https://doi.org/10.1016/j.arabjc.2016.09.020>.
- Naraginti, S., Li, Y.i., 2017. Preliminary investigation of catalytic, antioxidant, anticancer and bactericidal activity of green synthesized silver and gold nanoparticles using *Actinidia deliciosa*. *J. Photochem. Photobiol., B* 170, 225–234.
- Ocsoy, I., Tasdemir, D., Mazicioglu, S., Celik, C., Kati, A., Ulgen, F., 2018. Biomolecules incorporated metallic nanoparticles synthesis and their biomedical applications. *Mater. Lett.* 212, 45–50.
- Oueslati, M.H., Tahar, L.B., Harrath, A., 2020. Catalytic, antioxidant and anticancer activities of gold nanoparticles synthesized by kaempferol glucoside from *Lotus leguminosae*. *Arabian J. Chem.* 13 (1), 3112–3122. <https://doi.org/10.1016/j.arabjc.2018.09.003>.
- Paiva-Santos, A.C., Herdade, A.M., Guerra, C., Peixoto, D., Pereira-Silva, M., Zeinali, M., Mascarenhas-Melo, F., Paranhos, A., Veiga, F., 2021. Plant-mediated green synthesis of metal-based nanoparticles for dermatopharmaceutical and cosmetic applications. *Int. J. Pharm.* 597, 120311. <https://doi.org/10.1016/j.ijpharm.2021.120311>.
- Pantidos, N., Horsfall, L.E., 2014. Biological synthesis of metallic nanoparticles by bacteria, fungi and plants. *J. Nanomed. Nanotechnol.* 5, 1.
- Parveen, A., Rao, S., 2015. Cytotoxicity and genotoxicity of biosynthesized gold and silver nanoparticles on human cancer cell lines. *J. Cluster Sci.* 26 (3), 775–788.
- Perween, T., Mandal, K., Hasan, M., 2018. Dragon fruit: An exotic super future fruit of India. *J. Pharmacogn. Phytochem.* 7, 1022–1026.
- Ramírez Castro, J., García-Hernández, L., Ramírez Ortega, P.A., Arenas Islas, D., 2018. Green synthesis of gold nanoparticles (AuNPs) by *Cupressus goveniana* extract. *ECS Trans.* 84 (1), 207–215.
- Rebecca, O., Boyce, A.N., Chandran, S., 2010. Pigment identification and antioxidant properties of red dragon fruit (*Hylocereus polyrhizus*). *Afr. J. Biotechnol.* 9 (10), 1450–1454.
- Rehman, M., Ullah, S., Bao, Y., Wang, B.o., Peng, D., Liu, L., 2017. Light-emitting diodes: whether an efficient source of light for indoor plants? *Environ. Sci. Pollut. Res.* 24 (32), 24743–24752.
- Salem, S.S., EL-Belely, E.F., Niedbala, G., Alnoman, M.M., Hassan, S.-D., Eid, A.M., Shaheen, T.I., Elkeliish, A., Fouda, A., 2020. Bactericidal and in-vitro cytotoxic efficacy of silver nanoparticles (Ag-NPs) fabricated by endophytic actinomycetes and their use as coating for the textile fabrics. *Nanomaterials* 10 (10), 2082. <https://doi.org/10.3390/nano10102082>.
- Santhoshkumar, J., Rajeshkumar, S., Venkat Kumar, S., 2017. Phyto-assisted synthesis, characterization and applications of gold nanoparticles—A review. *Biochem. Biophys. Rep.* 11, 46–57.
- Sathishkumar, P., Gu, F.L., Zhan, Q., Palvannan, T., Mohd Yusoff, A.R., 2018. Flavonoids mediated 'Green'nanomaterials: A novel nanomedicine system to treat various diseases—Current trends and future perspective. *Mater. Lett.* 210, 26–30.
- Sati, S.C., Kour, G., Bartwal, A.S., Sati, M.D., 2020. Biosynthesis of Metal Nanoparticles from Leaves of *Ficus palmata* and Evaluation of Their Anti-inflammatory and Anti-diabetic Activities. *Biochemistry* 59 (33), 3019–3025.
- Selim, M.E., Hendi, A.A., 2012. Gold nanoparticles induce apoptosis in MCF-7 human breast cancer cells. *Asian Pac. J. Cancer Prev.* 13 (4), 1617–1620.
- Sergiev, I., Todorova, D., Shopova, E., Jankauskiene, J., Jankovska-Bortkevič, E., Jurkonienė, S., 2019. Exogenous auxin type compounds amend PEG-induced physiological responses of pea plants. *Sci. Hortic.* 248, 200–205.
- Simonis, F., Schilthuisen, S., 2006. Nanotechnology; Innovation Opportunities for Tomorrow's Defence, Report TNO Science & Industry Future Technology Center, the Netherlands.
- Singh, H., Du, J., Singh, P., Yi, T.H., 2018. Ecofriendly synthesis of silver and gold nanoparticles by *Euphrasia officinalis* leaf extract and its biomedical applications. *Artificial Cells, Nanomed. Biotechnol.* 46 (6), 1163–1170.
- Slepička, P., Slepičková Kasálková, N., Siegel, J., Kolská, Z., Švorčík, V., 2020. Methods of gold and silver nanoparticles preparation. *Materials.* 13 (1). <https://doi.org/10.3390/ma13010001>.
- Suganthy, N., Ramkumar, V.S., Pugazhendhi, A., Benelli, G., Archunan, G., 2018. Biogenic synthesis of gold nanoparticles from *Terminalia arjuna* bark extract: assessment of safety aspects and neuroprotective potential via antioxidant, anticholinesterase, and antiamyloidogenic effects. *Environ. Sci. Poll. Res.* 25,10418–33.
- Syafinar, R., Gomeş, N., Irwanto, M., Fareq, M., Irwan, Y., 2015. FT-IR and UV-VIS spectroscopy photochemical analysis of dragon fruit. *ARPJ J. Eng. Appl. Sci.* 10, 6354–6358.
- Talbot, G.H., Bradley, J., Edwards, J.E., Gilbert, D., Scheld, M., Bartlett, J.G., 2006. Bad bugs need drugs: an update on the development pipeline for the Antimicrobial Availability Task Force of the Infectious Diseases Society of America. *Clin. Infect. Dis.* 42 (5), 657–668.
- Unal, I.S., Demirbas, A., Onal, I., Ildiz, N., Ocsoy, I., 2020. One step preparation of stable gold nanoparticle using red cabbage extracts under UV light and its catalytic activity. *J. Photochem. Photobiol., B* 204, 111800. <https://doi.org/10.1016/j.jphotobiol.2020.111800>.
- Utpott, M., Ramos de Araujo, R., Galarza Vargas, C., Nunes Paiva, A.R., Tischer, B., de Oliveira, Rios A, et al., 2020. Characterization and application of red pitaya (*Hylocereus polyrhizus*) peel powder as a fat replacer in ice cream. *Journal of Food Processing and Preservation.* 44 (5). <https://doi.org/10.1111/jfpp.14420>.
- Vandermeer, C., 2020 Promising natural extracts for use in active food packaging: ResearchSpace@ Auckland.
- Veerakumar, K., Govindarajan, M., Rajeswary, M., Muthukumar, U., 2014. Low-cost and eco-friendly green synthesis of silver nanoparticles using *Feronia elephantum* (Rutaceae) against *Culex quinquefasciatus*, *Anopheles stephensi*, and *Aedes aegypti* (Diptera: Culicidae). *Parasitol. Res.* 113 (5), 1775–1785.
- Velidandi, A., Pabbathi, N.P.P., Dahariya, S., Baadhe, R.R., 2020. Catalytic and eco-toxicity investigations of bio-fabricated monometallic nanoparticles along with their anti-bacterial, anti-inflammatory, anti-diabetic, anti-oxidative and anti-cancer potentials. *Colloid Interface Sci. Commun.* 38, 100302. <https://doi.org/10.1016/j.colcom.2020.100302>.
- Vijayan, R., Joseph, S., Mathew, B., 2018. Indigofera tinctoria leaf extract mediated green synthesis of silver and gold nanoparticles and assessment of their

- anticancer, antimicrobial, antioxidant and catalytic properties. *Artif. Cells Nanomed. Biotechnol.* 46 (4), 861–871. <https://doi.org/10.1080/21691401.2017.1345930>.
- Wali, M., Sajjad, A., Sumaira, S., Muhammad, N., Safia, H., Muhammad, J., 2017. Green synthesis of gold nanoparticles and their characterizations using plant extract of *Papaver somniferum*. *Nano Sci Nano Technol.* 11, 118.
- Waris, A., Din, M., Ali, A., Ali, M., Afridi, S., Baset, A., Ullah Khan, A., 2021. A comprehensive review of green synthesis of copper oxide nanoparticles and their diverse biomedical applications. *Inorganic Chemistry Communications.* 123, 108369. <https://doi.org/10.1016/j.inoche.2020.108369>.
- Wu, M., Feng, Q., Sun, X., Wang, H., Gielen, G., Wu, W., 2015. Rice (*Oryza sativa* L) plantation affects the stability of biochar in paddy soil. *Sci. Rep.* 5, 1–10.
- Wu, L.-C., Hsu, H.-W., Chen, Y.-C., Chiu, C.-C., Lin, Y.-I., Ho, J.-A., 2006. Antioxidant and antiproliferative activities of red pitaya. *Food Chem.* 95 (2), 319–327.
- Youssif, K.A., Haggag, E.G., Elshamy, A.M., Rabeh, M.A., Gabr, N.M., Seleem, A., Salem, M.A., Hussein, A.S., Krischke, M., Mueller, M.J., Abdelmohsen, U.R., Mukherjee, A., 2019. Anti-Alzheimer potential, metabolomic profiling and molecular docking of green synthesized silver nanoparticles of *Lampranthus coccineus* and *Malephora lutea* aqueous extracts. *PLoS ONE* 14 (11), e0223781. <https://doi.org/10.1371/journal.pone.0223781>.
- Zayadi, R.A., Abu Bakar, F., Ahmad, M.K., 2019. Elucidation of synergistic effect of eucalyptus globulus honey and *Zingiber officinale* in the synthesis of colloidal biogenic gold nanoparticles with antioxidant and catalytic properties. *Sustainable Chem. Pharm.* 13, 100156. <https://doi.org/10.1016/j.scp.2019.100156>.

Further Reading

- Sarfraz, N., Khan, I., 2021. Plasmonic Gold Nanoparticles (AuNPs): Properties, Synthesis and their Advanced Energy, Environmental and Biomedical Applications. *Chem. – Asian J.* 16 (7), 720–742. <https://doi.org/10.1002/asia.202001202>.